1·0

2·8

2·5

5·0

3·15

2·2

5·6

3·5

1·1

7·1

4·0

2·0

4·5

1·8

1·25

1·4

1·6

NATIONAL BUREAU OF STANDARDS
MICROCOPY RESOLUTION TEST CHART
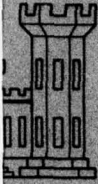
DREDGED MATERIAL RESEARCH PROGRAM

FREEZE-THAW ENHANCEMENT OF THE DRAINAGE AND CONSOLIDATION OF FINE-GRAINED DREDGED MATERIAL IN CONFINED DISPOSAL AREAS

by

Edwin J. Chamberlain, Scott E. Blouin

Foundations and Materials Research Branch
U. S. Army Cold Regions Research and Engineering Laboratory
Hanover, New Hampshire 03755

October 1977

Final Report

Approved For Public Release; Distribution Unlimited

IN REPLY REFER TO: WESYV

10 October 1977

SUBJECT: Transmittal of Technical Report D-77-16

TO: All Report Recipients

1. The report transmitted herein represents the results of a study of a dredged material dewatering concept evaluated as part of Task 5A (Dredged Material Densification) of the Corps of Engineers' Dredged Material Research Program (DMRP). This task is part of the Disposal Operations Project of the DMRP and is concerned with developing and/or testing promising techniques for dewatering or densifying (i.e., reducing the volume of) dredged material using physical, biological, and/or chemical techniques prior to, during, and/or after placement in containment areas.

2. The rapidly escalating requirements for land for the confinement of dredged material, often in urbanized areas where land values are high, indicated that significant priority within the DMRP be given to research aimed at extending the useful life of existing or proposed containment facilities. While increased life expectancy can be achieved to some extent by improved site design and operation and to a greater extent by removing dredged material for use elsewhere, the attractive approach being considered under Task 5A is to densify the in-place dredged material. Densification of the material would not only increase site capacity but would also result in an area that was more attractive for various subsequent uses because of the improved engineering properties of the material.

3. The objective of this study (Work Unit 5A07) was to investigate the volume reduction of dredged material obtained through natural freezing and thawing processes. The study consisted of laboratory tests of dredged material obtained from disposal sites in the Great Lakes region. The investigation was conducted by the Foundation and Materials Research Branch of the U. S. Army Cold Regions Research and Engineering Laboratory, Hanover, New Hampshire.

4. Fine-grained dredged material was subjected to controlled freeze-thaw cycling in a special laboratory consolidometer. Volume changes and permeabilities were observed after full consolidation and after freeze-thaw cycling at various applied pressures. It was observed that as much
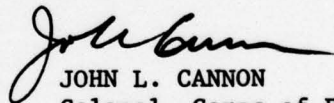
as 20 percent or more additional volume reduction resulted when dredged
material with liquid limit in the range of 60 to 90 was subjected to one
cycle of freezing and thawing. The degree of overconsolidation by
freezing and thawing appears to decrease with increasing amounts of
coarse material and with increasing plasticity. The vertical permeability
of all materials examined was increased as much as two orders of magnitude,
with the greatest increased in permeability occurring for fine-grained
material at the lowest stress level.

5. The application of the phenomenon of overconsolidation by freezing
and thawing to disposal site management is discussed and site management
procedures are suggested. The process appears to be particularly adapt-
able to regions of severe winters where material frost penetrations of
more than 1 m can be obtained, but it could be applied in regions of
more moderate winters such as in the Great Lakes region by sequentially
depositing and freezing dredged material during the winter months.

6. It should be emphasized that the conclusions drawn in this report
are based on the results of laboratory studies. It was not within the
scope of the study to conduct large-scale field investigations. The
reliability of extrapolating laboratory freeze-thaw consolidation and
permeability data to field situations is unproven. At present, it is
felt that the overall management of a site should consider additional
volume that may be gained through the freeze/thaw phenomenon. This
study did not, however, include investigation of detailed designs for
water removal during the thaw period, which would have to be handled on
a case-by-case basis.

JOHN L. CANNON
Colonel, Corps of Engineers
Commander and Director

Unclassified

SECURITY CLASSIFICATION OF THIS PAGE (When Data Entered)

REPORT DOCUMENTATION PAGE		READ INSTRUCTIONS BEFORE COMPLETING FORM
1. REPORT NUMBER Techincal Report D-77-16	**2. GOVT ACCESSION NO.**	**3. RECIPIENT'S CATALOG NUMBER**
4. TITLE (and Subtitle) FREEZE-THAW ENHANCEMENT OF THE DRAINAGE AND CONSOLIDATION OF FINE-GRAINED DREDGED MATERIAL IN CONFINED DISPOSAL AREAS.		**5. TYPE OF REPORT & PERIOD COVERED** Final report, May 75-Apr 76, **6. PERFORMING ORG. REPORT NUMBER**
7. AUTHOR(s) Edwin J. Chamberlain Scott E. Blouin		**8. CONTRACT OR GRANT NUMBER(s)** Interagency Agreement WESRF 75-102236-T
9. PERFORMING ORGANIZATION NAME AND ADDRESS U. S. Army Cold Regions Research and Engineering Laboratory, Foundations and Materials Research Branch, Hanover, N. H. 03755		**10. PROGRAM ELEMENT, PROJECT, TASK AREA & WORK UNIT NUMBERS** DMRP Work Unit No. 5A07
11. CONTROLLING OFFICE NAME AND ADDRESS Office, Chief of Engineers, U. S. Army Washington, D. C. 20314		**12. REPORT DATE** Oct 1977 **13. NUMBER OF PAGES** 85
14. MONITORING AGENCY NAME & ADDRESS(if different from Controlling Office) U. S. Army Engineer Waterways Experiment Station Environmental Effects Laboratory P. O. Box 631, Vicksburg, Miss. 39180		**15. SECURITY CLASS. (of this report)** Unclassified **15a. DECLASSIFICATION/DOWNGRADING SCHEDULE**

16. DISTRIBUTION STATEMENT (of this Report)

Approved for public release; distribution unlimited

J7. DISTRIBUTION STATEMENT (of the abstract entered in Block 20, if different from Report)

18. SUPPLEMENTARY NOTES

19. KEY WORDS (Continue on reverse side if necessary and identify by block number)

Consolidation (Soils)	Fine-grained soils
Drainage	Freeze-thaw tests
Dredged material	Permeability
Dredged material disposal	

20. ABSTRACT (Continue on reverse side if necessary and identify by block number)

Fine-grained dredged material obtained from disposal sites in the Great Lakes region was subjected to controlled freeze-thaw cycling in a special laboratory consolidometer. Volume changes and permeabilities were observed after full consolidation and freeze-thaw cycling for applied pressures in the range of 0.93 to 30.73 kPa. It was observed that as much as 20 percent or more volume reduction results when dredged material with liquid limits in the range of 60 to 90 percent is subjected to one cycle of freezing and thawing. The degree of

(Continued)

DD FORM 1473 1 JAN 73   EDITION OF 1 NOV 65 IS OBSOLETE

Unclassified

SECURITY CLASSIFICATION OF THIS PAGE (When Data Entered)

20. ABSTRACT (Continued).

overconsolidation by freezing and thawing appears to decrease with increasing amounts of coarse materials and with increasing plasticity. The vertical permeability of all materials examined was increased as much as two orders of magnitude, the greatest increase in permeability occurring for the fine-grained materials at the lowest stress levels. The application of the phenomenon of overconsolidation by freezing and thawing to disposal sites is discussed and site management procedures are suggested. The process appears to be particularly adaptable to regions of cold winters where material frost penetrations of more than 1 m can be obtained, but it can be applied to regions of more moderate winters such as in the Great Lakes region by sequentially depositing and freezing dredged material during the winter months.

PREFACE

The study reported herein was performed at the U. S. Army Cold Regions Research and Engineering Laboratory (CRREL) in Hanover, N. H., under Interagency Agreement WESRF 75-102236-T with the U. S. Army Engineer Waterways Experiment Station (WES), Vicksburg, Miss. This study forms Work Unit 5A07 of the Dredged Material Research Program (DMRP), administered by the Environmental Effects Laboratory (EEL).

The work was conducted during the period May 1975-April 1976. The principal investigators were Messrs. Edwin J. Chamberlain and Scott E. Blouin of the Foundations and Materials Research Branch, CRREL, Mr. Frederick Crory, Chief. This report was prepared by Messrs. Chamberlain and Blouin.

Special thanks are due to Dr. Anthony Gow for the thin-section studies and to the U. S. Army Engineer Districts, Buffalo, Detroit, and Chicago, for their assistance in obtaining dredged material samples.

During the conduct of the study, COL Robert Crosby was Commander and Director and Dr. Dean Freitag was Technical Director of CRREL. Mr. Albert Wuori was Chief, Experimental Engineering Division.

This study is part of WES EEL DMRP Task 5A, Dredged Material Densification, Dr. T. A. Haliburton, Manager, under the Disposal Operations Project, Mr. Charles C. Calhoun, Jr., Manager. Contract Manager was Mr. Michael Palermo, EEL. The study was under the general supervision of Dr. John Harrison, Chief, EEL.

Commanders and Directors of WES during the conduct of this study and preparation of the report were COL G. H. Hilt, CE, and COL J. L. Cannon, CE. Technical Director was Mr. F. R. Brown.

CONTENTS

LIST OF TABLES

LIST OF FIGURES

4

5

6

CONVERSION FACTORS, U. S. CUSTOMARY TO METRIC (SI)
UNITS OF MEASUREMENT

U. S. customary units of measurement used in this report can be converted to metric (SI) units as follows:

Multiply	By	To Obtain
feet	0.3048	metres
square feet	0.09290304	square metres
acres	4046.856	square metres
cubic feet	0.02831685	cubic metres
cubic yards	0.7645549	cubic metres
pounds (mass) per cubic foot	16.01846	kilograms per cubic metre
Btu (thermochemical) feet per hour square foot °F	1.7307	watts per metre-kelvin
Fahrenheit degrees	0.555	Celsius degrees or Kelvins*

---

* To obtain Celsius (C) temperature readings from Fahrenheit (F) readings, use the following formula: $C = (5/9)(F - 32)$. To obtain Kelvin (K) readings, use: $K = (5/9)(F - 32) + 273.15$.

FREEZE-THAW ENHANCEMENT OF THE DRAINAGE AND CONSOLIDATION OF FINE-GRAINED DREDGED MATERIAL IN CONFINED DISPOSAL AREAS

PART I: INTRODUCTION

Background

1. Environmental concern over open-water disposal of dredged material has created an increasing demand for disposal sites on land in the vicinity of harbors and water courses. However, because a large percentage of dredged material is fine grained and disposed of at high water contents, it makes poor fill material. Maximizing containment volume and improving the engineering properties of such material depend primarily on increasing its dry density and removing water. This densification process is especially difficult to achieve rapidly where the dredged material contains a significant proportion of clay soils.

2. At most Corps of Engineers (CE) disposal sites, no attempt has been made to enhance the natural densification processes other than to decant the supernatant over weirs. Other potentially more effective techniques, such as those employing internal drains, surcharges, well points, electro-osmosis, wicks, etc., are presently being evaluated under the Dredged Material Research Program (DMRP) at the U. S. Army Engineer Waterways Experiment Station (WES).

3. The study reported herein is of a more unconventional densification technique: freeze-thaw consolidation. This concept evolved from recent laboratory studies, which have shown that some soils can be overconsolidated by freeze-thaw cycling; that is, the bulk densities of certain soils can be increased by freeze-thaw cycling. For instance, the studies of Morgenstern and Smith (1973) show that a single freeze-thaw cycle on a clay soil with an applied pressure of 0.18 kgf/cm^{2*} resulted

---

* 1 kgf/cm^2 = 98.07 kPa/m^2.

8

in an overconsolidation equivalent to an applied pressure of approximately 0.62 kgf/cm^{2}[*] (Figure 1). Under field conditions, the increased density would be equivalent to that obtained by applying a surcharge of approximately 3 m of earth.
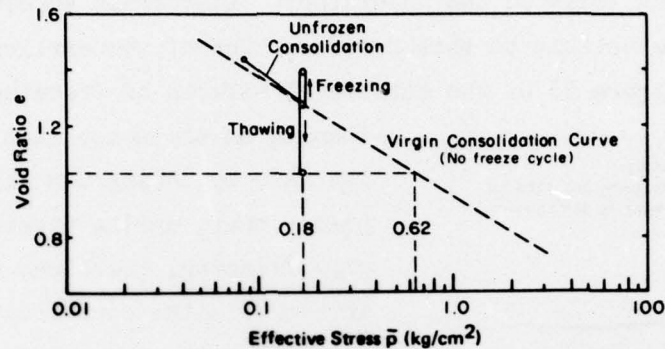
Figure 1. Void ratio-log effective stress
from Morgenstern and Smith (1973)

Purpose and Scope

4. The objective of this study was to determine the feasibility of using natural frost action to accelerate and enhance the consolidation of fine-grained dredged material so as to increase available containment volume and improve engineering properties. The study focused on a laboratory investigation of the influence of freezing and thawing on the consolidation properties of dredged material and the associated development and evaluation of the laboratory thaw consolidation apparatus. In addition, it included an informal survey of potential areas of application within the contiguous 48 states, the collection of representative samples of dredged material from these areas for laboratory evaluation, and an overall assessment of the potential for application of this method. This assessment combined the laboratory results with an estimate of the geographical and climatological limitations and the anticipated operational problems and peculiarities of actual study sites.

---

[*] For convenience, symbols and unusual abbreviations are listed and defined in Appendix B. Symbols used in figures, but not defined in text can also be found in Appendix B.

9

5. The phenomenon of preconsolidation resulting from freezing and thawing has been observed by many researchers in the course of consolidation of thawing soils in the laboratory. Clay soils appear to be particularly susceptible to this process. One of the earliest reported observations (Figure 2) of the beneficial effects of freezing and thawing on the consolidation of soil was made by Shusherina (1959), who reported that, during thawing after slow freezing, there was a significant increase in the consolidation of a clay loam, the increased consolidation being more pronounced at low applied pressures (0-0.5 kgf/cm^2) than at high applied pressures (>2 kgf/cm^2). Shusherina attributed the freeze-thaw
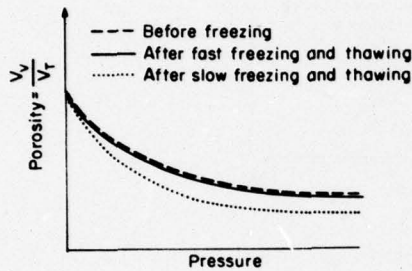
Figure 2. Consolidation of unfrozen and thawed loam according to Shusherina (1959)

consolidation increase to the dispersed structure formed during freezing and to an increase in permeability. Stuart (1964) also observed this preconsolidation effect in thawed clays (Figure 3). He suggested two possible mechanisms: one of disturbance and remolding brought about by freezing and thawing (similar to the explanation of Shusherina), and one of preconsolidation due to ice crystallization pressure. Stuart thought the latter was more probable. Ponomarev (1966) (Figure 4) made similar observations for a clay soil and suggested that the ice crystallization pressure brought about an aggregation and densification of clay particles that resulted in an increased permeability immediately upon thawing.
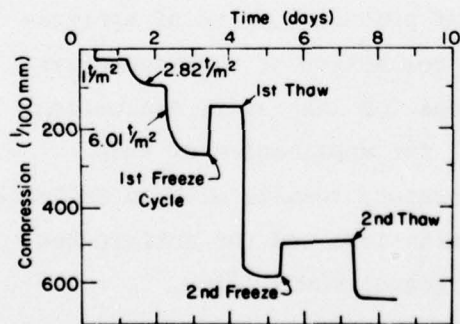
Figure 3. Thaw consolidation curve for a clay according to Stuart (1964)

6. Tsytovich et al. (1966) observed that the preconsolidation effect was dependent on the rate of thawing: the faster the thawing
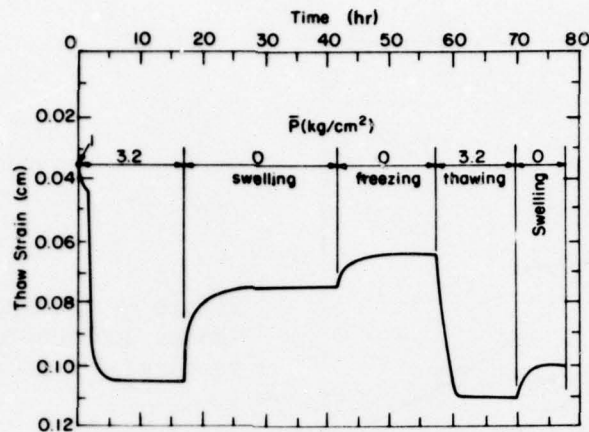
Figure 4.   Thaw consolidation for an
unknown soil according to Ponomarev
(1966)

rate, the more pronounced the consolidation.   Furthermore, they observed
that, if a clay soil thawed without a load and the load was subsequently
applied upon complete thawing, the preconsolidation effect would be sig-
nificantly less (Figure 5).   Tsytovich et al. (1966) described the
phenomenon as follows:

> During freezing dense mineral aggregates of mois-
> ture content (containing only unfrozen water) form
> with ice being, more or less, uniformly distributed in
> the voids between the aggregates.   Because of the high
> permeability of the aggregated structure water formed
> by the melting of the ice is easily squeezed out of
> the [thawing] soil even by a small load.   If no load
> is applied the water formed by the melting of the ice
> interacts with the surface of the mineral particles
> and is absorbed by the aggregates dehydrated during
> freezing, and the soil aggregates swell.   The faster
> the thawing and drainage occur, the less the swelling
> will be.

7.   Malyshev (1969) observed that the degree of preconsolidation
after freezing and thawing depends on the grain size and mineral types,
density, moisture content, structural bonding, and freezing and thawing
rates (Figure 6).   He observed that clayey sands or silts thawing under
2-3 kgf/cm^2 pressure would consolidate to their optimum density and that
saturated clays or silty clays would consolidate to a saturated void
ratio (e) equivalent to that of their plastic limits (PL).   Nixon and

11
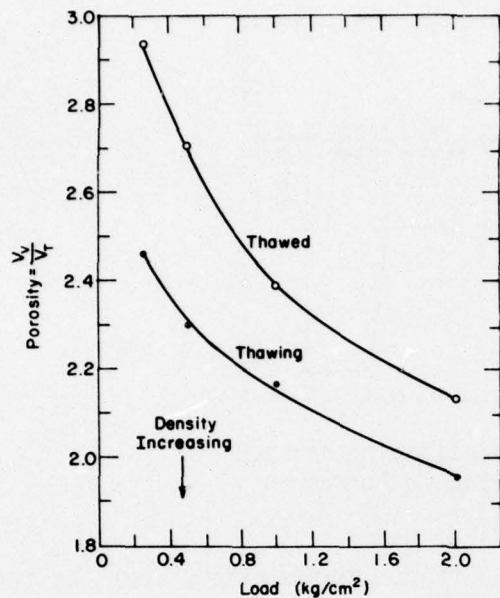
Figure 5. Consolidation of thawed and thawing clay according to Tsytovich (1966)

LOESS TYPE LOAM
Liquid Limit = 23.9
Plastic Limit = 15.3
% < 0.05 mm = 14.7 %
Unified Soil Classification: CL (inorganic clay of low to med. plasticity)
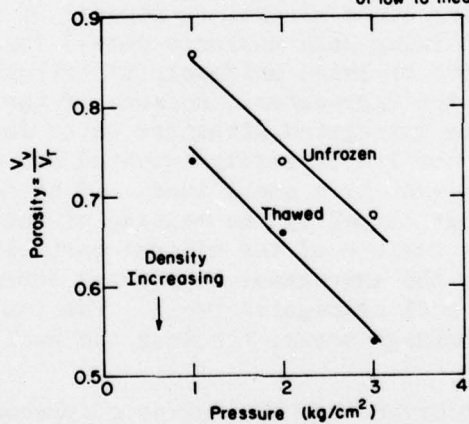
Figure 6. Consolidation of thawed load according to Malyshev (1969)

Morgenstern (1973) reported that the preconsolidation effect on silt and clay soils was enhanced by repeated freeze-thaw cycling, the additional consolidation after each cycle being smaller than after the previous cycle (Figure 7). They demonstrated that in the void ratio vs log

12
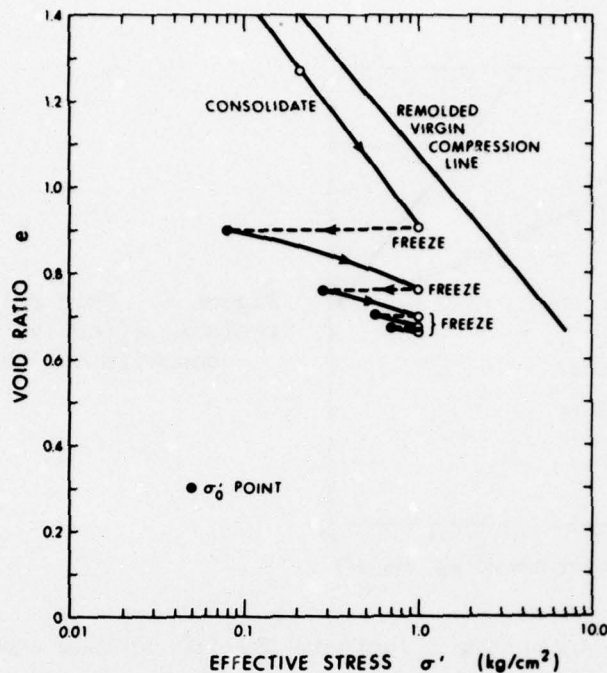
Reproduced by permission of the National Research Council
of Canada from the Canadian Geotechnical Journal, Volume
10, pp 571-580, 1973.

Figure 7. The measurement of residual
stress for reconstituted Athabasca
clay (Nixon and Morgenstern 1973)

effective stress plane there exists a locus of points defining the lim-
its of consolidation due to freezing and thawing. For two clay soils
and one silt, the lines thus defined were straight, falling below the
virgin consolidation curve and appearing to intersect the virgin curve
at high effective stresses (Figure 8).

Mechanism of Freeze-Thaw Consolidation

8. From the literature review, it can be concluded that the freeze-
thaw overconsolidation effect is brought on by:

a. Aggregation and/or restructuring of soil particles.

b. Densification of the aggregates.

c. Segregation of ice.

The resulting structure may or may not include ice lenses, but it is
necessary that ice be segregated.

13
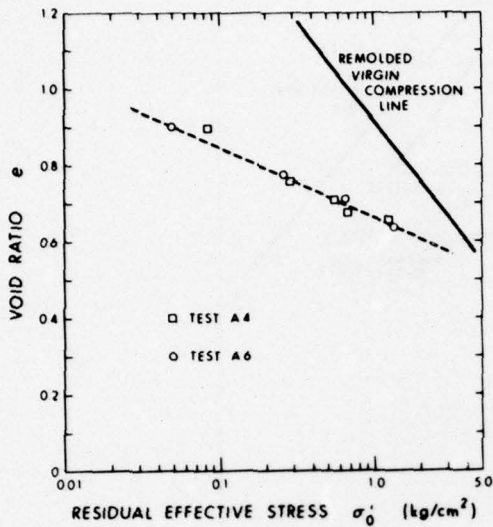
Figure 8. Void ratio plotted with residual effective stress for re-constituted Athabasca clay

9. In order to better illustrate the freeze-thaw consolidation phenomenon, a freeze-thaw cycle for a typical clay soil is depicted in Figure 9 on the plot of void ratio vs stress. Two representations of
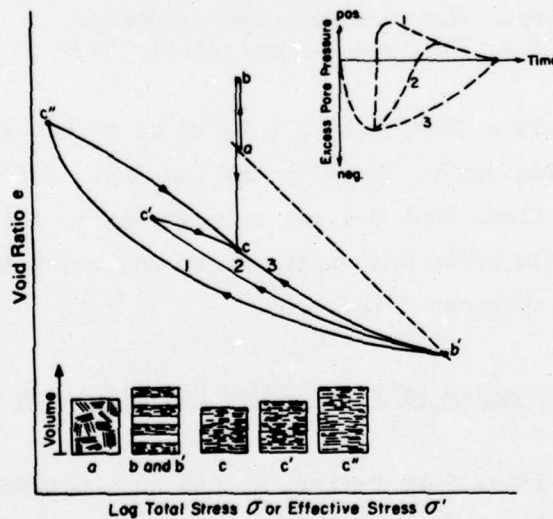
Figure 9. Theorized thaw consolidation process

the stress path are shown: the first as a function of total stress p and the second as a function of effective stress $\bar{p}$. (Effective stress is defined as the total stress minus the pore water pressure.) These

14

stress paths are superimposed on the virgin consolidation curve for the clay in the unfrozen-undisturbed condition.

10. It is assumed that prior to freezing the material is saturated with water and normally consolidated to point a on the virgin consolidation curve (Figure 9). All excess pore water pressure has been dissipated. Freezing is unidirectional and water is free to flow as in nature. The initial soil structure is illustrated schematically as flocculated and the excess pore water pressure is zero for the normally consolidated condition at point a (see inserts, Figure 9). In terms of total stress, the stress path is vertical as the material heaves from point a to point b, due to moisture migration and to the expansion of water to ice during freezing. Freezing causes a restructuring of the clay into a more compact, dispersed, and layered (or aggregated) structure (insert b and b', Figure 9), with each clay layer (or aggregate) bounded by ice. The resulting frozen structure has been termed by Martin (1959) as "rhythmically banded."

11. This segregation of ice from soil has been observed by many investigators of frost action in soils. The soil layers consist of mineral particles, unfrozen water, air, and possibly some ice. The bulk of the ice, however, is formed in lenses bounding the clay layers. Large negative pore pressures developing at the freezing front draw water from between the clay particles, resulting in the formation and densification of lenses or aggregations of clay particles.

12. Upon thawing, the total stress path is vertical and the material consolidates from point b to point c. This structure is depicted in insert c as being more dispersed and compact. The net effect is an overconsolidation of the material.

13. The process can be better presented in terms of effective stress. Reference is again made to the void ratio–log stress diagram in Figure 9 and the inserts for soil structure and pore pressure. A clay slurry is fully consolidated to point a on the virgin compression curve and frozen with free access to water. Externally, the sample has undergone a net increase in void ratio to point b due to the expansion of water to ice and the intake of water from the reservoir. However,

15

during freezing discrete elements of clay and ice have formed, the clay elements being overconsolidated to point b' due to the negative pore water pressures. Schematically, the structure has changed from the dispersed form shown in insert a to the segregated and flocculated form shown in insert b and b'. Upon thawing the effective stress path within the discrete elements of clay is depicted along line b'-c to point c where the pore pressures are in equilibrium with the applied load, and the material has undergone a net decrease in void ratio from point a to point c.

14. For the bulk sample, the effective stress path during thawing is dependent upon the relationship between the rate of generation of melt water and the combined rates of drainage and adsorption of water by the clay aggregates. On one extreme is the case where thawing is instantaneous and little or no drainage or adsorption occurs during thawing. In this case (curve 1, Figure 9), the excess pore water pressure generated may equal or nearly equal the applied stress, the effective stress falling to or nearly to zero along the path b'-c". The volume decrease from point b to point c" can be accounted for by the ice-water volume change. With the passage of sufficient time, the excess pore water pressure goes to zero, as water drains away and the effective stress resumes the value of the total applied stress at point c. On the other extreme, the rate of thawing is slower than the combined rates of drainage and adsorption. In this case (curve 3), no excess pore water pressure is generated during thawing and the material swells to point c. In between these extremes (curve 2), drainage and adsorption rates are somewhat slower than the thawing rate. Excess pore water pressures are generated as the material swells to point c', a significant volume change occurring. Upon completion of thawing, the material consolidates to point c as excess pore pressures are dissipated.

Application of the Freeze-Thaw Consolidation Phenomena to Fine-Grained Dredged Material

15. Thus, it is suggested that the freeze-thaw consolidation process may be applicable to consolidating fine-grained dredged material.

But dredged material often contains organic and chemical matter, and the effectiveness of the freeze-thaw consolidation process on these materials is unknown. However, conditioning (dewatering) of highly organic sewage and paper mill sludge by freezing and thawing has been found to be effective by numerous investigators (Bishop and Fulton 1968, Bruce et al. 1953, Clements et al. 1950, Doe et al. 1965, Farrell et al. 1970, Katz and Mason 1970, and Noda et al. 1964). For instance, Clements et al. (1950) found that freezing and thawing acted as a flocculent in sewage sludge with a high moisture content and accelerated the rate of sludge settling. The end product was clear water and aggregations of particles that settled out. Furthermore, Doe et al. (1965) reported the experience of a full-scale pilot plant which exploited the freeze-thaw dewatering process. The concentrated solid matter, however, was in the form of a gel which could not sustain significant loads. Disposal was in land fills where an earth surcharge was used to bring about densification. It is not clear whether any attempts were made by Doe et al. (1965) to further concentrate the sewage gel by freeze-thaw consolidation.

PART II: INVESTIGATION

Sites Visited

16.   In order to evaluate the feasibility of employing freeze-thaw consolidation in the field, a number of sites in the Great Lakes area in New York, Ohio, Michigan, Illinois, and Wisconsin were visited. A review of the climatology of the 48 contiguous United States had showed that the Great Lakes area is the only region in the country where natural freezing of dredged material has potential application. There are extensive dredging operations in the area under the control of CE Districts headquartered at Buffalo, Detroit, and Chicago. Operations are concerned chiefly with channel maintenance in the lakes themselves and in the rivers and harbors serving the highly industrialized areas along the south and west shores of the lakes. Most dredged material deposited in containment areas comes from the river and harbor channel maintenance and is principally fine grained, silt and clay sized, and somewhat contaminated. The fine grain sizes make the material difficult to dewater but well suited for freeze-thaw enhanced consolidation.

Sample collections

17.   Material samples were collected from a total of 10 disposal areas. All sites were diked containment areas with weir facilities to control runoff. Some of the sites were in diked areas onshore, while others were diked areas offshore. The offshore sites either had one or more sides against the shore or were man-made islands encircled by dikes. The areas chosen were representative of most containment areas in the Great Lakes, both from geographical and material properties standpoints. Samples were collected from two sites in Buffalo, New York: Times Beach and the Small Boat Harbor; two sites in Toledo, Ohio: Penn 7 and an offshore diked island in Maumee Bay; one site in Monroe, Michigan: on the River Rasin; one site in Detroit, Michigan: Grassy Island; two sites in Chicago, Illinois: O'Brien Lock and the 122nd Street and Stoney Island site; and one site in Green Bay, Wisconsin: the Bay Port disposal area. Sizes of the sites varied

from approximately 1×10^5 m^2 for the smaller sites at Buffalo and Toledo to 16×10^5 m^2 for the Bay Port area in Green Bay.

18. A sample was also obtained from the St. Marys River in Sault St. Marie, Michigan; however, this material was very coarse grained and not suitable for inclusion in this study.

General site descriptions

19. The containment areas are generally owned by State, county, or local governments or will be turned over to them when filled. In some instances (Penn 7 in Toledo, for example), the areas are owned by corporations. In most cases it is difficult to envision practical uses of these containment areas when filled without extensive dewatering and/or overlayment with stable fill material. The difficulty, as noted previously, is that the dredged material is predominantly fine grained with a high water content and low permeability. As the surface dries, it forms a crust, and material beneath the crust usually remains at high water content. Thus, bearing capacity, even after years of drying and settlement, remains very low. A view of typical crust formation is shown in Figure 10. The crust is laced with tensile cracks produced by

Figure 10. Typical crust formation at 122nd St. and Stoney Island site in Chicago

19

shrinkage during the drying process. It measured 0.15 m thick and resulted from more than 2 years of drying. The crust would support a man but would not support nonbuoyant vehicles.

20. Typically, dredged material is pumped from the dredge through a pipe (usually 0.45 m or larger) into the containment area. Material is deposited according to grain size as the effluent fans outward from the pipe outlet. Cobbles and boulders are deposited at the outlet, followed in turn by gravels, sands, and fines further away. As a result, the elevation of the dredged material changes gradually throughout the containment area. It is highest near the pipe outlet, sloping gently away toward the outlet weir. In most of the areas surveyed, granular materials made up only a small percentage of the dredged material and hence covered only small portions of the containment areas. Figure 11 shows the pipe outlet at the Small Boat Harbor site in Buffalo surrounded by cobbles and boulders. Another view looking away from the pipe is shown in Figure 12. The soil rapidly grades to fines and is incapable of supporting a man beyond about 45 m from the outlet. It slopes gently away from the pipe, falling below the water table in more distant portions of the containment area.

21. The changes in soil gradation are shown in Figures 13-15, taken at the Times Beach disposal area in Buffalo. Figure 13 shows a silty clay approximately 75 m from pipe outlet, about as far as one could safely walk. Figure 14 shows a relatively clean sand and gravel approximately 15 m from the outlet, and Figure 15 shows cobbles, bricks, and other debris intermixed with gravel about 6 m from the outlet.

22. In none of the areas visited was the pipe outlet moved throughout the site to distribute granular material. While such an operation would be difficult and time-consuming with present equipment and procedures, it might be beneficial from the viewpoint of improving the average engineering properties of a site, particularly in areas where a significant amount of the material is granular. Generally, management of the containment areas is minimal, consisting of monitoring the weirs and moving the pipe only when elevation differences within an area dictate. In some areas intermediate dikes allow one portion of the total

20

Figure 11.   Outlet pipe at the Small Boat Harbor site
in Buffalo

Figure 12.   Looking away from outlet pipe at Small Boat
Harbor site

21
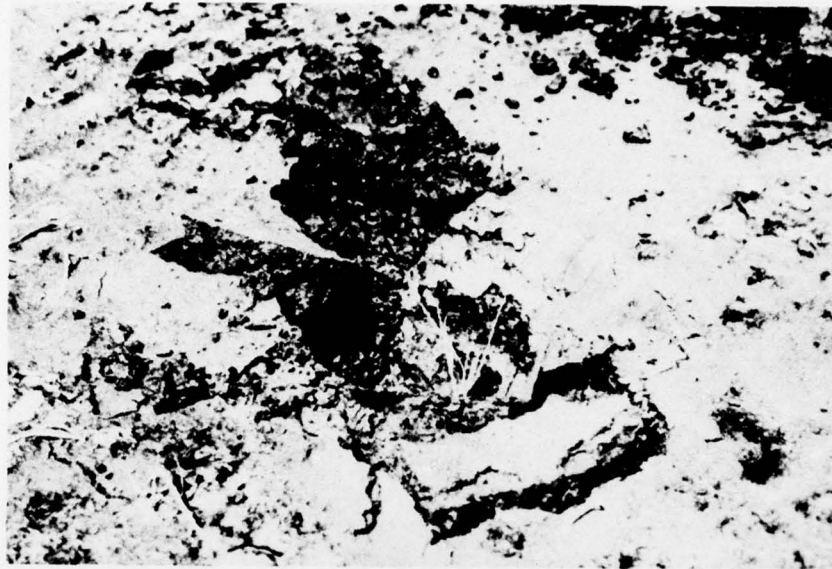
Figure 13. Silty clay area at Times Beach disposal area
in Buffalo

Figure 14. Clean sand and gravel area at Times Beach
disposal area

22

Figure 15. Cobbles, bricks, and debris at Times Beach
disposal area

area to be filled at a time. Adjacent portions are filled by moving the
pipe or switching to other branches of it.

23. It was observed that most sites had a propensity for vegeta-
tion. Within a single year grass and brush had taken root, and substan-
tial trees were in evidence several years after deposition of fine-
grained material. A view of typical brush and tree growth is shown in
Figure 16, taken at the Small Boat Harbor site in Buffalo. Such vegeta-
tion may itself enhance consolidation and dewatering but could impede
deployment of additional dewatering schemes.

Material Properties

24. Approximately 10 kg of dredged material was obtained from
each of ten sites. These samples came from only one area of each site
and were not necessarily representative of the entire site. Each was
placed in a sealed container and shipped to the Cold Regions Research
and Engineering Laboratory (CRREL). Upon receipt they were thoroughly
mixed and sampled for index property evaluation.

23

Figure 16. Typical brush and tree growth at Small Boat
Harbor site

25. The liquid (LL) and plastic (PL) limits, plasticity index (PI),
natural water content (w), organic content (w_o), specific gravity of
solids (G_s), Unified Soil Classification designation, and grain-size
distribution for each material are given in Figure 17. Five of the ten
sites sampled were selected as being representative of fine-grained
dredged material and were further analyzed.

Apparatus

26. In order to make valid laboratory studies of the effects of
freezing and thawing on the consolidation properties of dredged material,
it was necessary to design and fabricate a special consolidation appara-
tus. The unique features desired included:

    a. Controllable unidirectional freezing and thawing.

    b. Controllable top and bottom drainage.

    c. Low side wall friction.

    d. Provision for measurement of temperature profiles.

    e. Provision for measurement of pore pressures.

27. Unidirectional freezing was necessary to simulate the natural
freezing conditions of an infinite plane. Freezing from all directions,

24
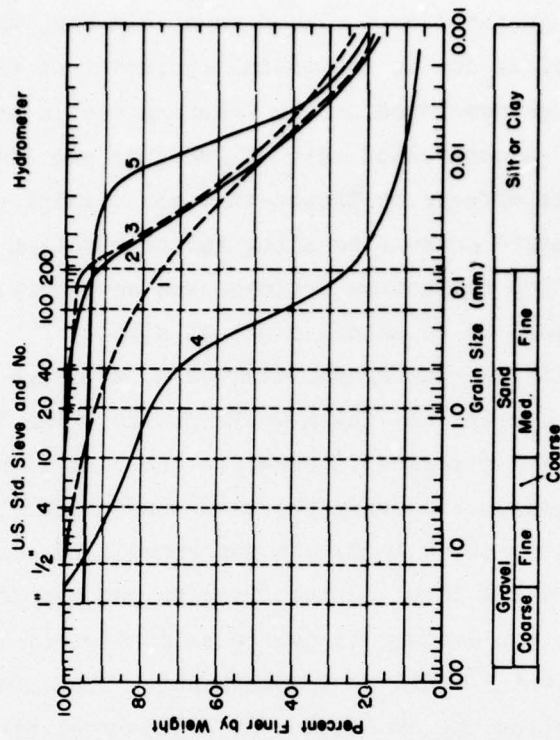
Curve No.	Site	G_s	Class.	w_o	w	LL	PL	PI
1	122nd & Stoney Isle	2.78	CL	2.3	58.1	37.3	21.9	15.4
2	Grassy Island	2.75	OH	9.6	64.3	60.7	34.9	25.8
3	Monroe	2.79	OH	6.9	70.7	79.3	41.3	38.0
4	Sault St. Marie	2.64	SM	0.2	20.8	13.3	NP	NP
5	Small Boat Harbor	2.73	OH	5.5	143.3	82.0	45.3	36.7
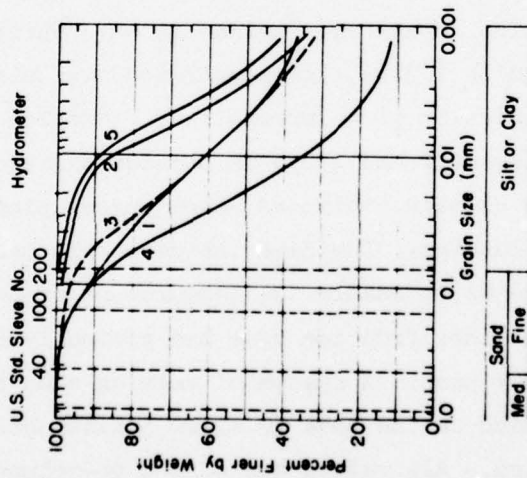
Curve No.	Site	G_s	Class.	w_o	w	LL	PL	PI
1	Toledo Penn 7	2.71	CH	3.8	74.9	61.3	27.8	33.5
2	O'Brien Lock	2.76	OH	5.3	95.3	89.2	42.0	47.2
3	Toledo Island	2.74	CH	2.9	108.7	70.7	29.6	41.1
4	Times Beach	2.80	ML	5.1	44.8	38.9	29.6	9.3
5	Green Bay	2.69	OH	9.2	268.5	198.0	59.6	138.4

Figure 17. Grain-size distribution and index properties of dredged material samples

25

such as would result if the apparatus were placed in a cold box, would cause unnatural stress conditions due to the radial restraint of the confining chamber (the stresses developed during freezing are in the direction of the heat flow). A controlled rate of freezing and thawing was desirable to evaluate rate effects on freeze-thaw consolidation enhancement, with the temperature sensors to allow the observation of freezing and thawing rates. Top and bottom drainage was necessary, again to simulate the conditions of an actual disposal site.

28. A low-friction confining chamber was desired to minimize side friction forces on the test material and the movable piston. The tests were to be run under low applied stresses to simulate the condition of little or no surcharge. Minimizing the side friction would ensure that the test material received the applied load. It was especially necessary that friction remain at a low level during freezing, as sample side friction and piston restraint would cause an overconsolidation of the test material, the amount of which would be indeterminate. The measurement of pore pressure would allow the evaluation of piston restraint, a very important factor as was observed in preliminary tests, and would allow the calculation of effective stress, which is important for understanding the mechanism of freeze-thaw consolidation enhancement.

29. The thaw consolidation apparatus, similar to an apparatus employed by Morgenstern and Smith (1973), is illustrated schematically in Figure 18. It consists basically of a Teflon-lined Plexiglas cylinder with a 63.5-mm inside diameter and 152.4-mm outside diameter. The fixed base and movable piston contain stainless steel porous plates with provisions for drainage and flushing. The base drainage line leads directly to a pressure transducer to enable the measurement of pore water pressure. The drainage lines from the base and piston lead to a constant head device and rotary pump. A system of valving also provides for a head of water to be placed on the base to allow falling head permeability tests to be conducted. All valves are of the no-volume-change type.

30. Both the base and piston contain thermoelectric cooling devices for controlled unidirectional freezing. By controlling the

26

Figure 18. Freeze-thaw consolidation apparatus
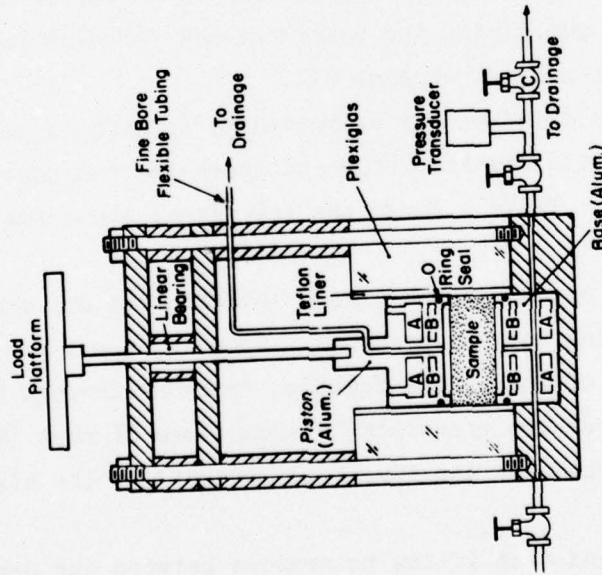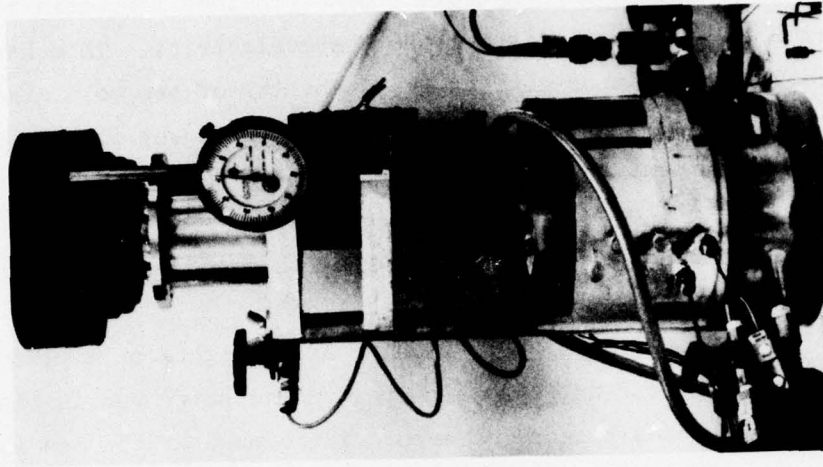
A. Heat Exchange Chamber for Water Circulation
B. Thermoelectric Cooling Devices
C. No Volume Change Valve

27

circulating water temperature and the power to the thermoelectrics, good control of the frost penetration rate can be obtained. Step changes in the base or piston thermoelectrics can be brought about by changing the input power. The constant temperature bath provided long-term stable heat removal from the hot sides of the thermoelectrics. This heat-removal mechanism is important, as the stability of the cold side depends on the stability of the warm side, with the power input controlling only the temperature difference between the two sides.

31. During the experiments, the temperature profile during freezing was obtained by observing the output of thermocouples positioned in the base, piston, and side wall of the cylinder.

32. The load was applied by placing dead weights on a piston guided by a linear bearing. (An air-operated actuator was initially used but was abandoned because of errors introduced at the low stress levels employed.)

33. The piston was sealed by means of a rubber O-ring. Other seals were investigated, but all resulted in a high piston friction. Piston seal friction using the O-ring was minimized by precise machining of the Teflon bore, minimizing the compressional force on the O-ring, and lubricating with a light machine oil.

34. The piston friction was evaluated by applying a known load on the chamber filled with deaired water and observing the pore pressure transducer response. Table 1 shows the frictional characteristics of the system used.

35. It can be seen that the piston friction did not vary significantly with increasing applied pressure. However, there was some scatter. The deviation of the piston friction from the average value as a percentage of the pressure transducer response was highest (8 percent) at lowest applied pressures and lowest (1 percent) at the highest applied pressures.

36. It was found that if the tolerances between the O-ring and the Teflon bore were further reduced, the friction could also be further reduced; however, leaks developed. Careful checks were made to evaluate the repeatability of the friction forces. Consistent results were

28

Table 1

Piston Friction Analysis

Applied Pressure on Piston kPa	Pressure Transducer Response kPa	Piston Friction kPa	Deviation of Piston Friction from Average	
			kPa	Percent of Transducer Response
5.11	2.83	2.28	+0.24	8
9.04	7.11	1.93	-0.11	2
16.91	14.77	2.14	+0.10	1
32.57	30.78	1.79	-0.25	1
		Avg 2.04		

obtained when care was employed in cleaning the Teflon bore, O-ring,
and piston, and when a sufficient amount of lubrication was applied.

37. A dial gage was used to observe the piston movement, and an
electrically operated rectilinear transducer was used to make a contin-
uous record. The outputs of the rectilinear transducer, the pressure
transducer, and the thermistors were recorded on strip chart recorders.
The output of the pressure transducer was also observed on a digital
voltmeter.

38. Figure 18 shows a closeup view of the freeze-thaw consolida-
tion apparatus. An overview of the apparatus and accessories is shown
in Figure 19.
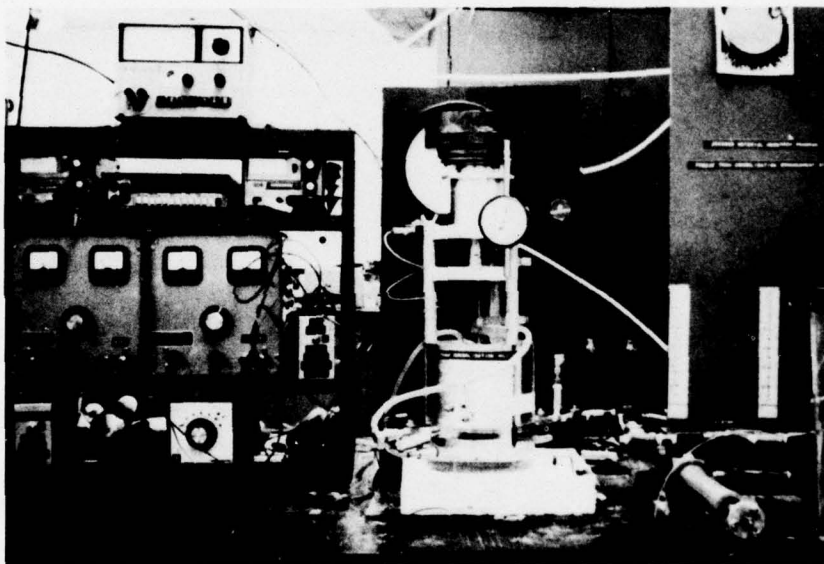
Figure 19.   Overview of the freeze-thaw
consolidation setup

Experimental Procedure

39. The test material was prepared by mixing the material thor-
oughly in a blender at a water content two to three times its LL. Both
the apparatus and the test material were deaired by applying a vacuum,
and the apparatus was filled with deaired water to approximately the

1-cm depth. A paper filter was placed on the base; a thermocouple inserted into the test chamber 3 mm above the base; and the deaired slurry poured into the chamber to a depth of approximately 30 mm. A filter paper was placed on the surface of the slurry and deaired water poured on top. A second filter was then placed on top to ensure that no fines entered the piston, and the piston was inserted. The piston was pushed into the cylinder until air bubbles ceased coming out of the connecting line and the connection was made to the drainage system. The desired load was then applied and the pore water pressure measured.

40. After application of the load, the sample was allowed to consolidate until the pore pressure fell to zero. This usually coincided with the end of consolidation, as little secondary consolidation was observed.

41. When the sample was to be frozen, the piston was raised to approximately double the sample height, and bottom-up freezing commenced with water free to flow through the piston. Raising of the piston and bottom-up freezing were employed to minimize the restraint to heaving on the sample during freezing. In preliminary tests, it was observed that a pressure in excess of 30 kPa was required to remove a frozen sample from the Teflon cylinder. It was also observed that, because of differential thermal contraction, the piston friction increased during freezing. Subsequent tests showed that variation of these test procedures had considerable effect on the test results. Upon complete freezing of the sample, it was allowed to thaw uncontrolled with water free to flow to the constant head device. Consolidation was considered complete once the pore water pressure fell to zero. Normally, two or three freeze-thaw cycles were required to maximize the degree of thaw consolidation.

42. Upon completion of normal and thaw consolidation tests, a falling head permeability test was conducted. Figure 20 is a schematic diagram of the test apparatus. Deaired water was raised to a known elevation in the burette, with the base of the test sample open to the constant head device. The transducer pressure was recorded, the valve controlling the water flow through the piston opened, and the fall in transducer pressure observed with time. The following equation was

31

⊗ No volume change valve
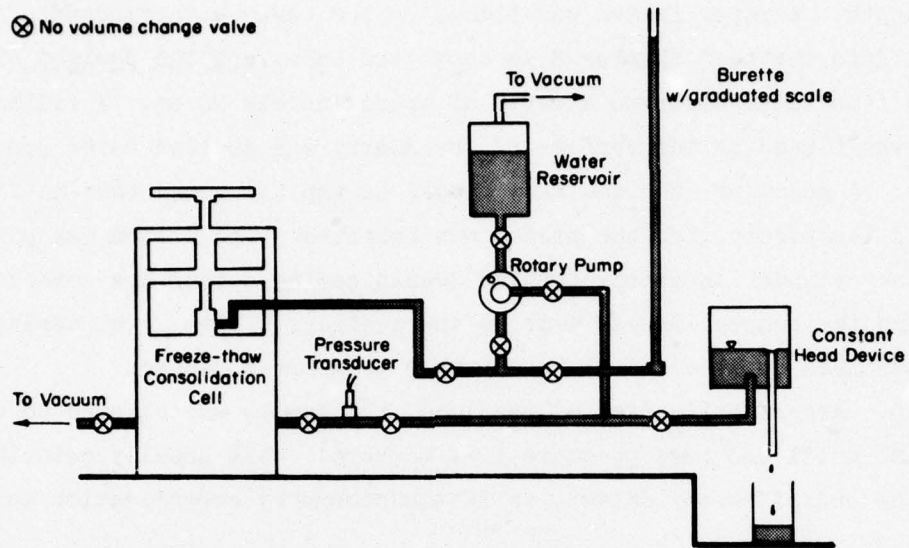
Figure 20. Schematic of permeability apparatus
used to calculate permeability k in meters per second:

$$k = 2.3 \, \frac{a}{A} \, \frac{H}{\Delta t} \, \log_{10} \frac{P_o}{P_f} \tag{1}$$

$$= 1.387 \times 10^{-2} \, \frac{H}{\Delta t} \, \log_{10} \frac{P_o}{P_f}$$

where

   a = area of burette = 19.1 mm^2

   A = area of sample = 3166.9 mm^2

   H = sample thickness (m)

   Δt = time interval (s)

   P_o = initial transducer pressure (kPa)

   P_f = final transducer pressure (kPa)

Test Results

43. Preliminary tests were conducted to evaluate the influence of
the direction of freezing. Figure 21 illustrates the results in the
void ratio vs effective stress plane for material obtained from the

32

Toledo Island site. The upper line represents the normally consolidated state. The numbers adjacent to the points indicate the number of freeze-thaw cycles; the direction of freezing is also noted. It can be seen that top-down freezing resulted in almost double the amount of overconsolidation at an applied stress of 1.0 kPa. As previously mentioned, extrusion forces in excess of 30 kPa were required to remove a frozen sample from the Teflon sleeve. If similar forces are mobilized during top-down freezing, the frozen plug would effectively cause an overconsoli-

Figure 21. Influence of the direction of freezing in void ratio-effective stress plane, Toledo Island site

dation of the unfrozen material beneath because of the resistance to heaving. However, during bottom-up freezing with the piston raised, the only restraint to heave was the adhesion of the unfrozen plug to the cylinder wall. The extrusion force for a thawed sample consolidated under the highest pressure of 30.7 kPa was 1.3 kPa, while thawed samples consolidated at 0.9 kPa fell from the cylinder under their own weight.

44. The rate of frost penetration appeared to be of little consequence within the range examined (Figure 22). For instance, the change in void ratio for the Toledo Island site material under an effective stress of 3.0 kPa was 28 percent after freezing at 381 mm/day, while the same material frozen at 33 mm/day underwent a void ratio change of 26 percent during thawing.

45. It appeared that a single freeze-thaw cycle was sufficient to produce at least 75 percent of the maximum densification possible with freeze-thaw cycling. This is illustrated in Figure 23, again for the Toledo Island material.

46. Table 2 shows the results for the five sites examined. In

33

Table 2

Summary of Freeze-Thaw Consolidation Test Results

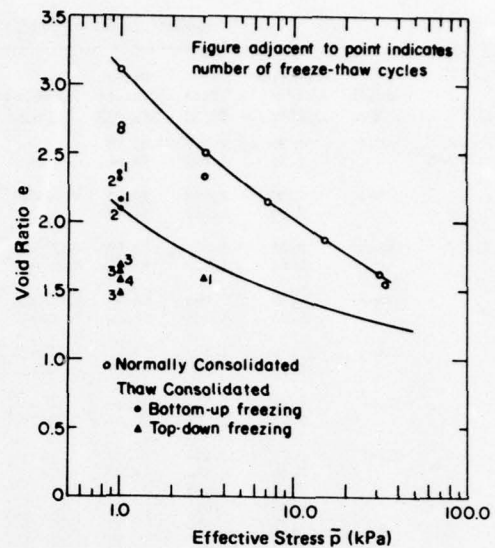| Site	Sample No.	Effective Stress kPa	Void Ratio	Water Content percent	Permeability m/s	Mode of Consolidation*	Frost Penetration Rate mm/day	Freezing Direction	Position of Piston	Comments
Toledo Island	TIS-1	2.80	2.338	88.78	-	Normal				
		2.80	1.803	68.46	-	1 f-t	280	Up	Raised	
	TIS-2	2.80	2.078	79.05	4.740×10^{-9}	Normal				
		2.80	1.493	56.79	-	1 f-t	380	Up	Normal	
	TIS-3	2.80	2.201**	83.69	8.020×10^{-9}	Normal				
		2.80	1.727	65.65	4.100×10^{-7}	1 f-t	200	Down	Normal	
	TIS-4	2.80	2.221	84.45	7.329×10^{-9}	Normal		Up	Normal	
		2.80	1.638	62.28	3.200×10^{-7}	1 f-t				
	TIS-5	30.73	1.502	57.11	1.370×10^{-9}	Normal				
		30.73	1.180	44.89	3.500×10^{-9}	1 f-t	130	Up	Normal	
	TIS-6	2.80	2.342	87.06	-	Normal		Down	Normal	
		2.80	1.588	59.04	9.70×10^{-8}	1 f-t	140			
	TIS-7	0.93	3.104	117.60	-	Normal				
		2.80	2.504	94.86	-	Normal				
		7.10	2.148	81.37	-	Normal				
		14.74	1.871	70.87	-	Normal				
		30.73	1.618	61.30	1.29×10^{-8}	Normal				
		30.73	1.332	50.45	1.80×10^{-8}	1 f-t	100	Up	Raised	
		30.73	1.270	48.13	3.28×10^{-8}	2 f-t	150	Up	Raised	
	TIS-8	0.93	2.690	102.29	1.82×10^{-9}	Normal				Recovery Time
		0.93	2.194	83.42	1.02×10^{-5}	1 f-t	150	Up	Raised	0.00 hr
		0.93	2.183	83.00	9.54×10^{-7}					0.13
		0.93	2.169	82.47	8.95×10^{-7}					0.50
		0.93	2.155	81.94	8.91×10^{-7}					22.22
		0.93	2.151	81.79	8.58×10^{-7}					23.30
		0.93	2.145	81.56	8.96×10^{-7}					64.63
		0.93	2.145	81.56	8.82×10^{-7}					64.68
		0.93	2.127	80.87	8.97×10^{-7}	2 f-t	150	Up	Raised	
		0.93	2.124	80.76	8.83×10^{-7}					
		0.93	1.689	64.22	4.93×10^{-7}	3 f-t	150	Up	Normal	
		0.93	1.483	56.37	-	4 f-t	210	Up	Normal	
	TIS-9	0.93	2.669	98.84	5.524×10^{-8}	Normal				
		0.93	2.356	87.27	2.345×10^{-6}	1 f-t	150	Up	Raised	
		0.93	2.307	85.44	2.500×10^{-6}	2 f-t	200	Up	Raised	
		0.93	1.654	61.24	9.206×10^{-8}	3 f-t	200	Down	Normal	
		0.93	1.579	58.48	1.138×10^{-7}	4 f-t	200	Down	Normal	
Toledo Penn 7	TP7-1	0.93	3.224	120.75	1.145×10^{-7}	Normal				
		2.80	2.457	92.02	2.509×10^{-8}	Normal				
		7.10	2.101	78.69	2.502×10^{-9}	Normal				
		14.72	1.841	68.95	2.514×10^{-9}	Normal				
		30.73	1.602	60.00	9.515×10^{-10}	Normal				
		30.73	1.242	46.52	1.416×10^{-9}	1 f-t	175	Up	Raised	
		30.73	1.116	41.80	4.875×10^{-9}	2 f-t	200	Up	Raised	
		30.73	1.116	41.80	3.989×10^{-9}	3 f-t	200	Up	Raised	
	TP7-2	2.80	2.377	89.02	9.866×10^{-9}	Normal				
		2.80	1.868	69.96	1.826×10^{-7}	1 f-t	200	Up	Raised	
		2.80	1.787	66.92	1.413×10^{-6}	2 f-t	200	Up	Raised	
	TP7-3	7.10	1.739	65.14	1.812×10^{-9}	Normal				
		7.10	1.448	54.22	6.582×10^{-7}	1 f-t	175	Up	Raised	
		7.10	1.428	53.50	7.959×10^{-7}	2 f-t	200	Up	Raised	
	TP7-5	1.37	2.622	98.20	1.298×10^{-8}	Normal				
		3.53	2.632	88.50	1.368×10^{-8}	Normal				
		7.65	2.073	77.64	4.319×10^{-9}	Normal				
		16.08	1.828	68.45	4.011×10^{-9}	Normal				
		32.75	1.457	54.56	6.274×10^{-10}	Normal				
		32.75	1.126	42.18	1.972×10^{-9}	1 f-t	175	Up	Raised	
		32.75	1.102	41.28	2.461×10^{-9}	2 f-t	175	Up	Raised	
	TP7-6	3.53	2.051	76.81	-	Normal				Delayed thaw consolidation (54 days)
		3.53	1.536	57.53	2.872×10^{-8}	1 f-t	200	Up	Raised	

(Continued)

*Freeze-thaw is abbreviated f-t.
**Incomplete consolidation as thermocouple probe interfered with piston.

Table 2 (Concluded)

| Site	Sample No.	Effective Stress kPa	Void Ratio	Water Content percent	Permeability m/s	Mode of Consoli-dation	Frost Penetration Rate mm/day	Freezing Direction	Position of Piston	Comments
Times Beach	TB-1	0.93	1.677	61.87	4.224×10^{-8}	Normal				
		2.80	1.528	56.40	2.582×10^{-8}	Normal				
		7.10	1.400	51.66	1.794×10^{-8}	Normal				
		14.72	1.274	47.01	1.327×10^{-8}	Normal				
		30.73	1.158	43.73	1.074×10^{-8}	Normal				
		30.73	1.081	39.89	6.841×10^{-8}	1 f-t	150	Up	Paised	
		30.73	1.081	29.89	1.429×10^{-7}	2 f-t	150	Up	Raised	
	TB-2	0.93	1.765	64.90	1.605×10^{-7}	Normal				
		0.93	1.852	68.08	2.997×10^{-6}	1 f-t	150	Up	Raised	
		2.80	1.636	60.14	1.458×10^{-6}					
		2.80	1.550	57.00	1.040×10^{-6}	2 f-t	175	Up	Raised	
		30.73	1.141	41.94	9.438×10^{-8}					
		30.73	1.074	39.47	1.678×10^{-7}	3 f-t	175	Up	Raised	
O'Brien Lock	OBL-1	0.93	3.225	121.90	1.208×10^{-8}	Normal				
		2.80	2.857	107.82	8.535×10^{-9}	Normal				
		7.10	2.453	92.57	-	Normal				
		14.74	2.148	79.52	3.836×10^{-9}	Normal				
		30.73	1.886	71.16	2.085×10^{-9}	Normal				
		30.73	1.516	57.21	-	1 f-t	200	Up	Raised	
		30.73	1.421	53.64	1.047×10^{-8}	2 f-t	200	Up	Raised	
		30.73	1.415	53.39	8.845×10^{-9}	3 f-t	200	Up	Raised	
	OBL-2	2.80	2.907	109.70	-	Normal				
		2.80	2.546	96.07	7.746×10^{-6}	1 f-t	225	Up	Raised	
		2.80	2.478	93.50	1.407×10^{-6}	2 f-t	200	Up	Raised	
		7.10	2.203	83.12	5.612×10^{-7}					
		14.74	1.934	73.00	1.044×10^{-8}					
		30.73	1.726	65.13	2.136×10^{-8}					
	OBL-3	7.10	2.533	91.78	6.027×10^{-9}	Normal				
		7.10	2.028	73.46	4.309×10^{-8}	1 f-t	200	Up	Raised	Recovery Time
		7.10	2.028	73.46	4.265×10^{-8}					
		7.10	1.999	72.43	2.056×10^{-7}	2 f-t	200	Up	Raised	0 days
		7.10	1.994	72.24	2.077×10^{-7}				Raised	0.07 days
		7.10	1.989	72.08	2.073×10^{-7}				Raised	0.19 days
		7.10	1.987	72.00	1.951×10^{-7}				Raised	0.84 days
		7.10	1.980	71.75	1.738×10^{-7}				Raised	2.90 days
		7.10	1.974	71.52	1.367×10^{-7}				Raised	5.08 days
		7.10	1.956	70.88	9.804×10^{-8}				Raised	7.08 days
		7.10	1.936	70.15	5.267×10^{-8}				Raised	9.94 days
		7.10	1.893	68.58	1.147×10^{-8}				Raised	17.18 days
		7.10	1.861	67.44	7.478×10^{-9}				Raised	24.17 days
		7.10	1.764	63.92	5.472×10^{-7}				Raised	53.12 days
Green Bay	GB-1	0.93	5.472	220.64		Partial				
		2.80	4.667	188.20	4.397×10^{-11}	Partial				
		2.80	4.408	177.73	8.897×10^{-9}	1 f-t	150	Up	Raised	
		2.80	4.536	182.91	3.502×10^{-9}	2 f-t	150	Up	Raised	
		2.80	4.335	174.79	6.026×10^{-9}	3 f-t	150	Up	Raised	

35
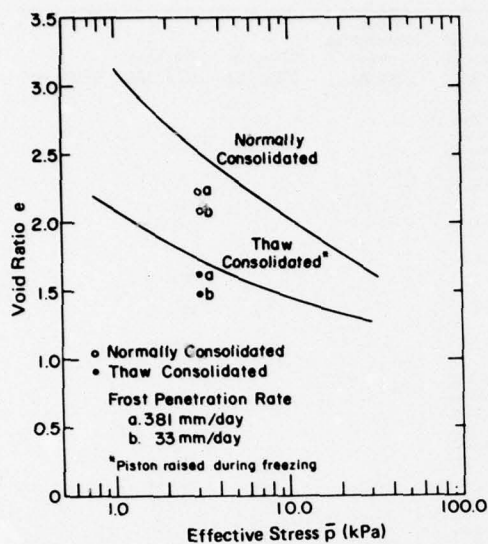
Figure 22. Influence of
frost penetration rate in
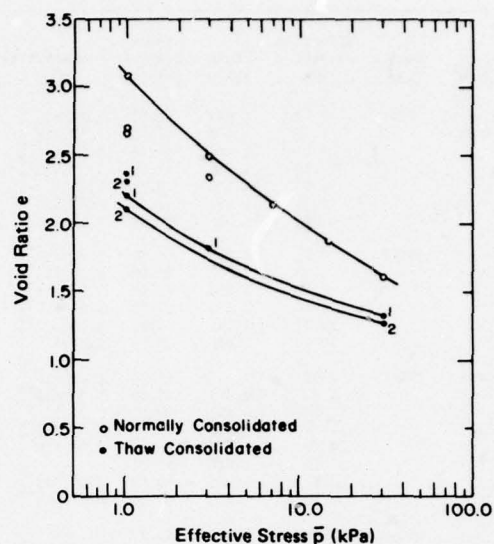void ratio-effective stress
plane, Toledo Island site

Figure 23. Void ratio-
effective stress for
the Toledo Island site
material

addition, plots in the void ratio vs effective stress plane are given
in Figures 23-27. The greatest degree of overconsolidation was observed
for the Toledo Island (Figure 23), Penn 7 (Figure 25), and O'Brien Lock
(Figure 26) materials that had plasticity indices of 41.1, 33.5, and
47.2 percent, respectively.

47. Freeze-thaw cycling was not an effective consolidation mech-
anism for all the materials tested. For instance, the void ratio vs
effective stress plot for the Buffalo Times Beach material was changed
little by freeze-thaw cycling (Figure 24). In fact, the void ratio for
this material increased after freeze-thaw cycling at the lower stress
levels. The change in void ratio for the Green Bay material (Figure 27)
was only 7 percent for the one test conducted, considerably lower than
the other materials. It must be concluded that materials of low plastic-
ity, such as the Buffalo Times Beach material, and materials of very
high plasticity, such as the Green Bay material, cannot be significantly
overconsolidated by freezing and thawing. This does not necessarily
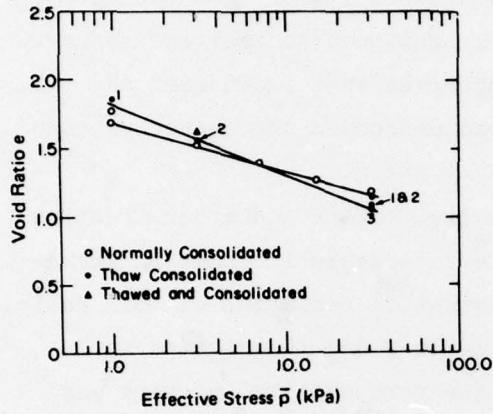mean that the Green Bay site is not suitable for application of this

36

Figure 24. Void ratio-effective stress for the Buffalo Times Beach material
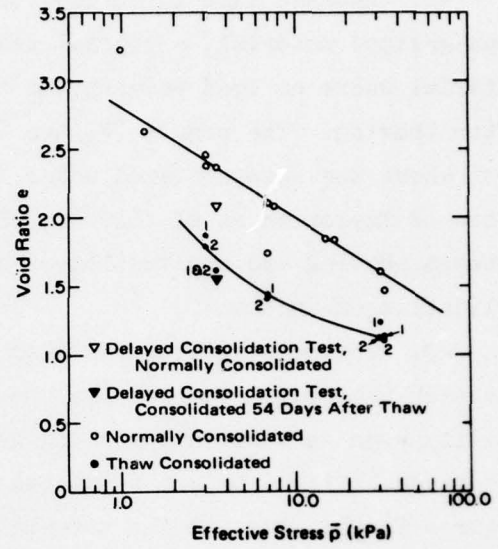

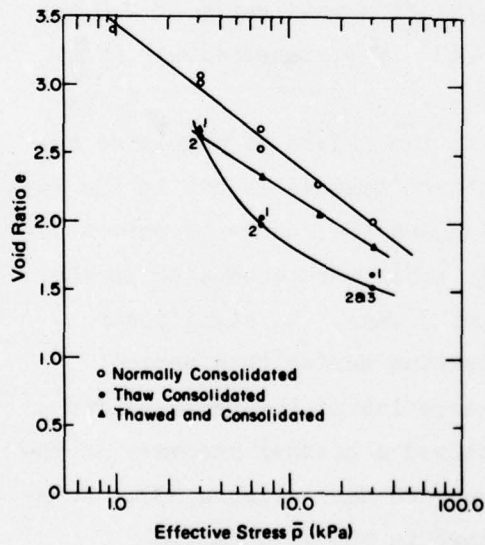Figure 25. Void ratio-effective stress for the Toledo Penn 7 material

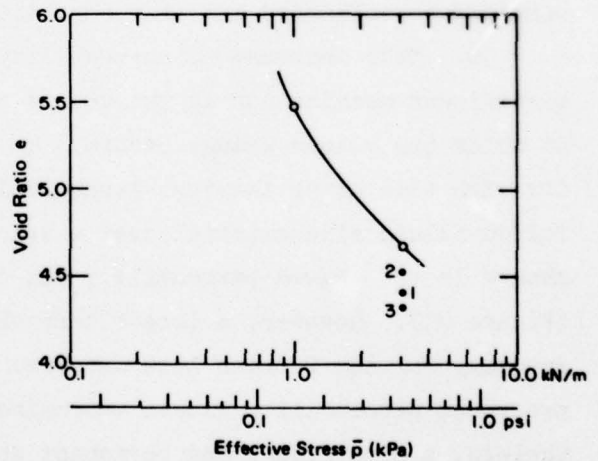Figure 26. Void ratio-effective stress for the O'Brien Lock material

Figure 27. Void ratio-effective stress for the Green Bay material

37

phenomenon, because the sample tested may not be representative as it was obtained from the corner of the site farthest from the outfall.

48. Because time is an important factor in the consolidation of fine-grained material, a special test was conducted on the Toledo Penn 7 material where no load was applied nor drainage allowed until 53 days after thawing. The result (Figure 25) differed little from the normal test where the sample thawed under load. This contradicts the observations of Tsytovich et al. (1966), who observed that increasing the time between thawing and application of a load decreased the degree of consolidation enhancement.

49. The permeability was also examined before and after freezing for each material. The results showed a remarkable increase in permeability even in materials showing a substantial reduction in void ratio. The permeability data are tabulated in Table 2 and illustrated in Figures 28-32. For all the materials, the permeability increase was greater at high void ratios than at low void ratios. For example, at a void ratio of 1.5, the normally consolidated permeability for the Toledo Island material (Figure 28) was approximately 1×10^{-9} m/s and the thaw-consolidated permeability was 1×10^{-7} m/s; at a void ratio of 2.0 the permeabilities were 4.6×10^{-9} and 7.6×10^{-7} m/s, respectively, for normally consolidated and thaw consolidated.

50. This increase of permeability of two orders of magnitude has significant meaning not in the volume changes achievable but in the rate at which the volume change occurs. To examine the change of permeability with time after thawing, permeability tests were conducted on the Toledo Island site material over a span of 3 days. No significant change in the thawed permeability was observed during this period (Figure 33). However, a longer term observation of the permeability recovery for the O'Brien Lock material showed a gradual recovery of the prefrozen permeability within approximately 20 days (Figure 33). Nonetheless, a significant and permanent change in the void ratio-permeability relationship occurred, as illustrated in Figure 31. It can be seen that the recovery curve lies between the normally consolidated and thaw-consolidated curves.

38

Figure 28. Permeability vs void ratio for the Toledo Island site material
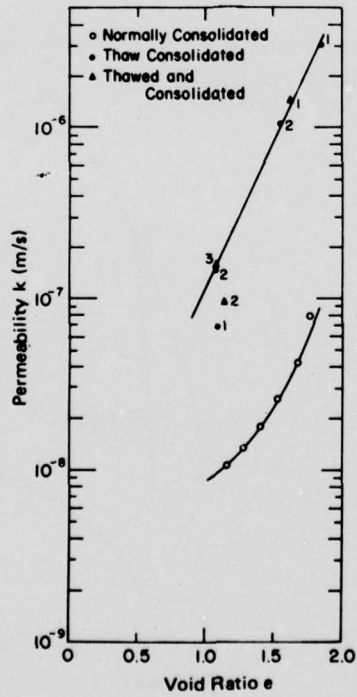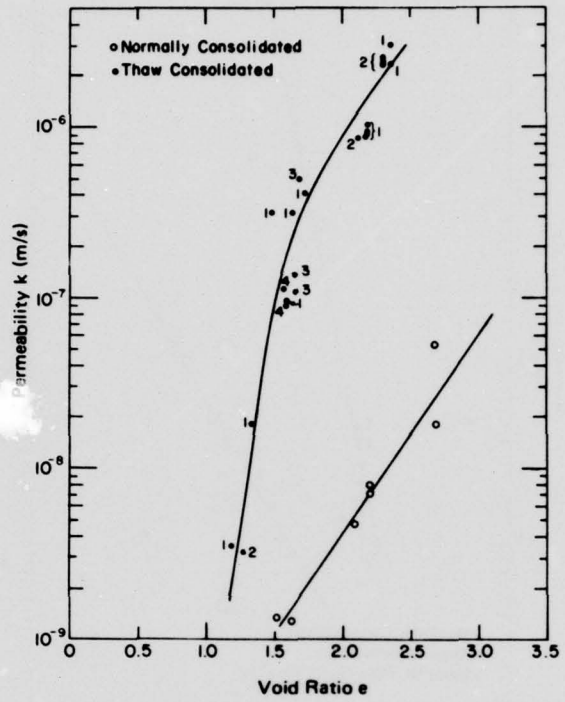

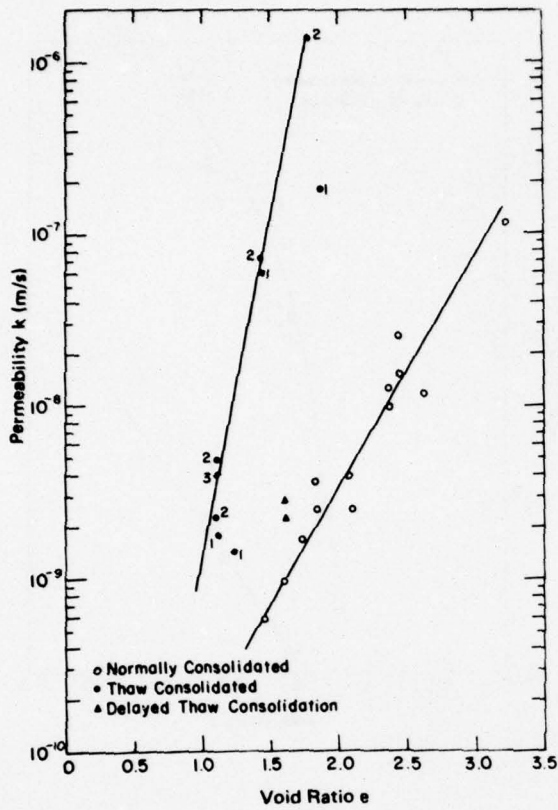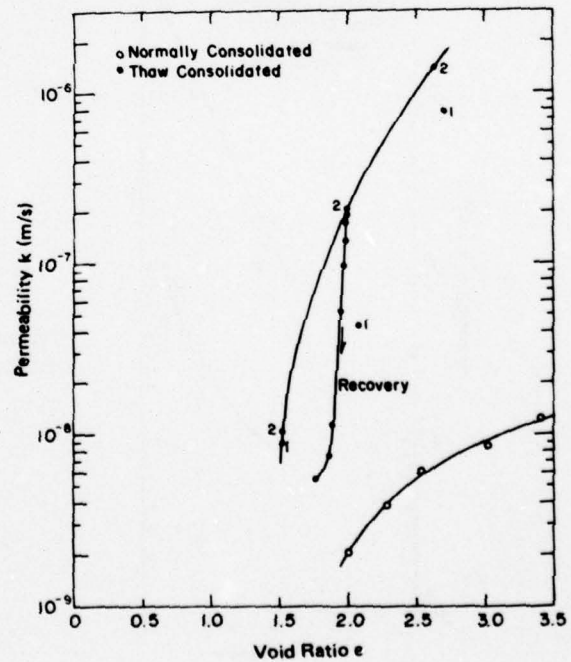Figure 29. Permeability vs void ratio for the Buffalo Times Beach material

39

Figure 30. Permeability vs void ratio for the Toledo Penn 7 material

Figure 31. Permeability vs void ratio for the O'Brien Lock material

40
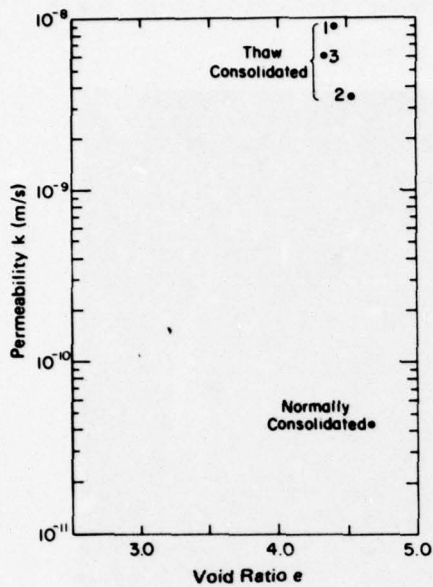
Figure 32. Permeability vs
void ratio for the Green Bay
material
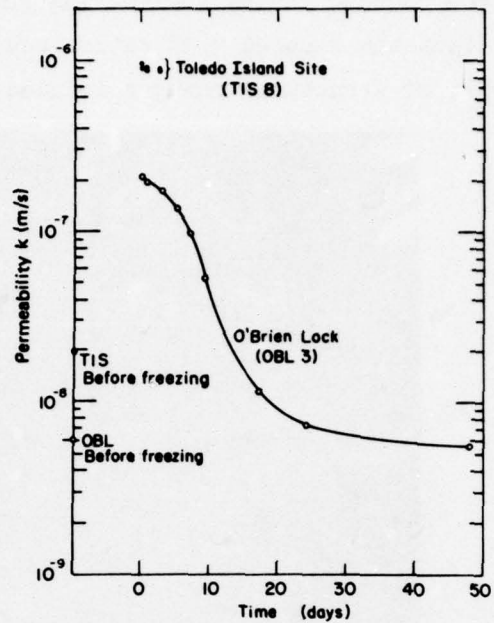
Figure 33. Permeability change
with time for the Toledo Island
and O'Brien Lock site material

51. The increased permeability can be readily understood by examining the specimens after freezing. For instance, Figure 34 shows the top surface of a Toledo Island sample after freezing and thawing but incomplete thaw consolidation. A polygonal structure is distinct, the boundaries of which become paths of least flow resistance. These features were not always visible to the naked eye after sample removal, particularly in the samples consolidated at the higher stress levels.

52. In order to more fully examine this structure, a thin-section study was made of the Toledo Penn 7 material after freezing. Figures 35 and 36 show 7× and 28× magnifications of a vertical profile. The dark areas are composed of dredged material solids and the light bands are ice. This illustrates distinctly the ice segregation that occurs during freezing. More remarkable are the 7× and 28× magnifications (Figures 37 and 38) of the horizontal thin sections that distinctly show the polygonal features previously observed in the unfrozen state.

53. These observations clearly substantiate that freezing can

41

induce changes in the engineering properties of fine-grained material
and that the reduced void ratios and increased permeabilities are a
result of structural changes induced by freezing.
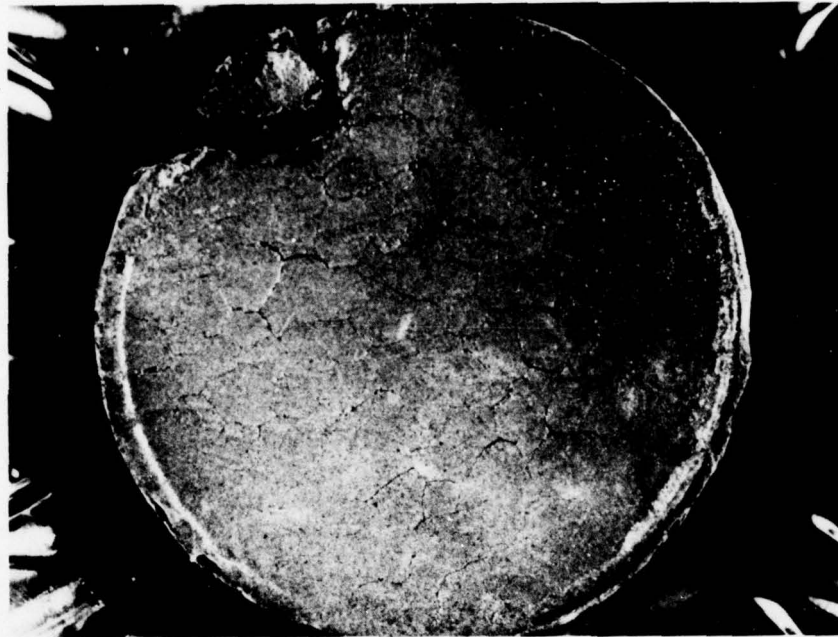
Figure 34.   Surface of Toledo Island sample TIS-3
after incomplete thaw consolidation
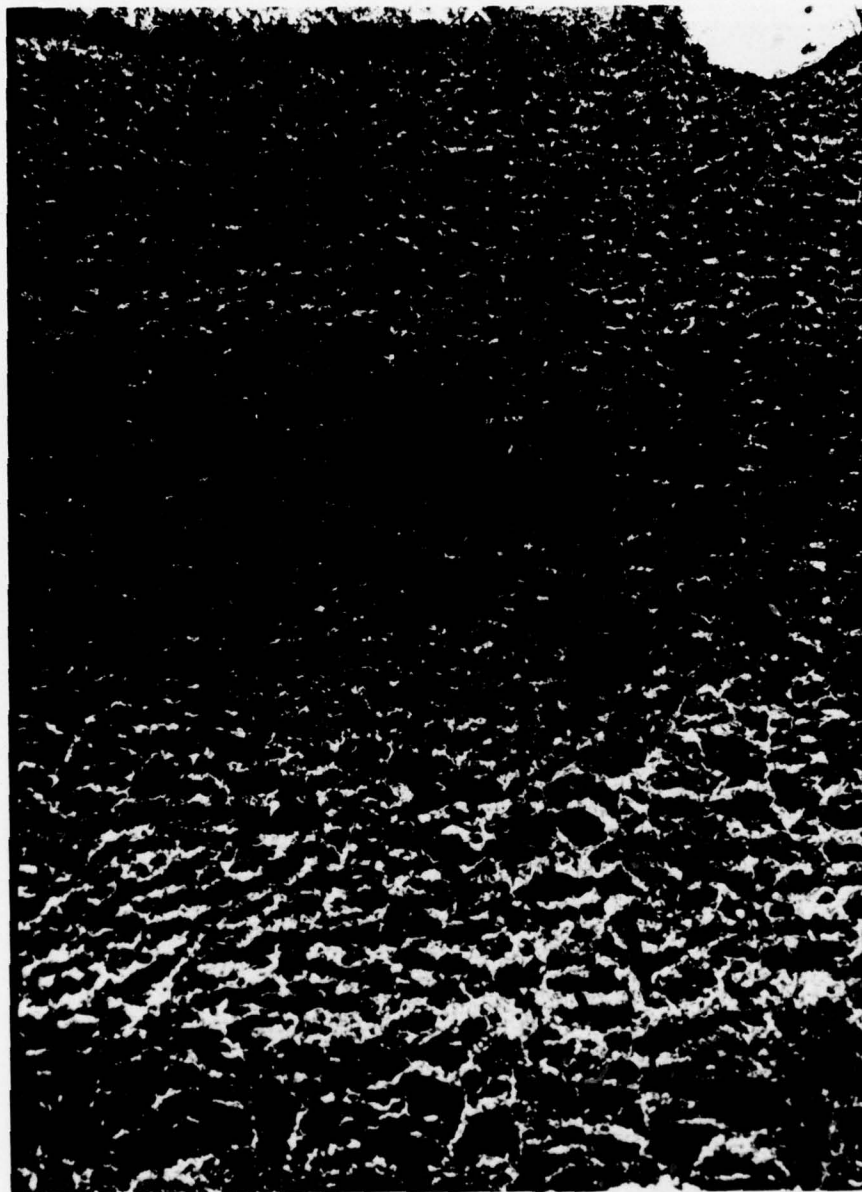
Figure 35. Magnification of 7× of a vertical thin section
of the Toledo Penn 7 material after freezing

43

Figure 36. Magnification of 28× of a vertical thin section
of the Toledo Penn 7 material after freezing
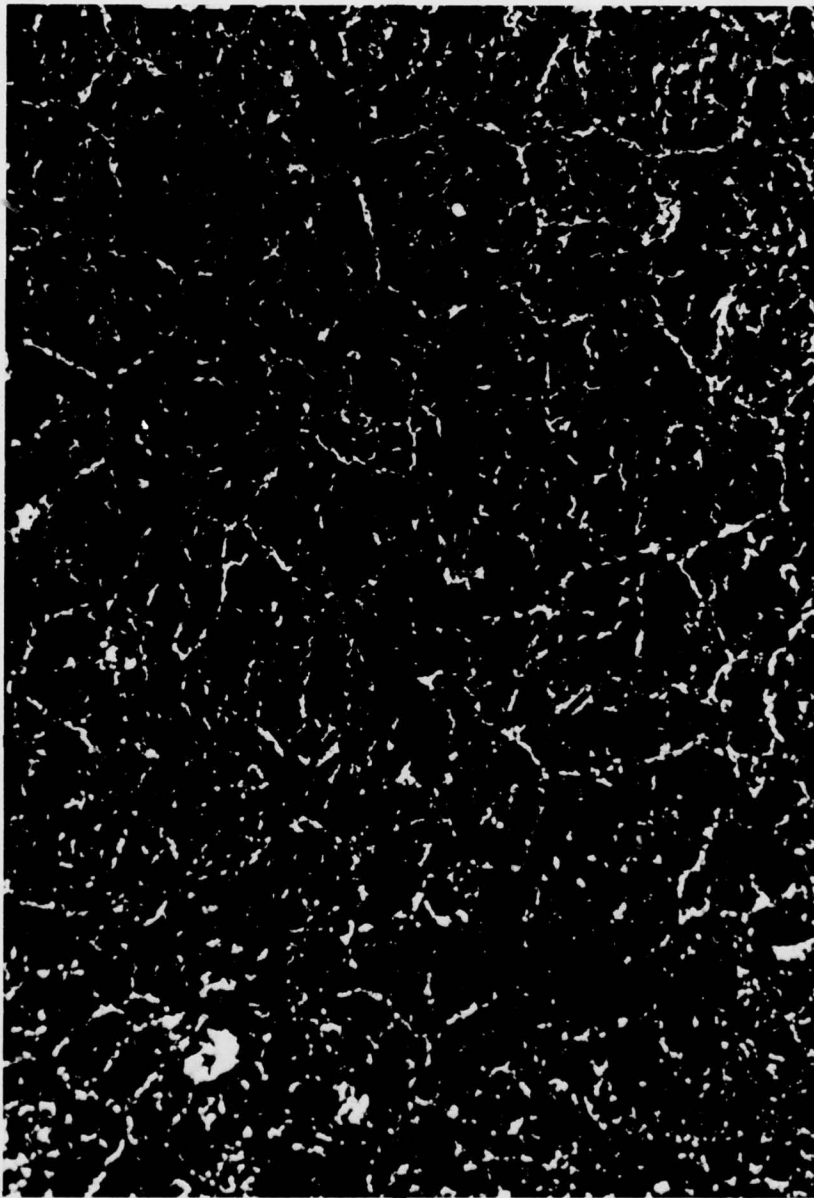
Figure 37. Magnification of 7× of a horizontal thin section
of the Toledo Penn 7 material after freezing
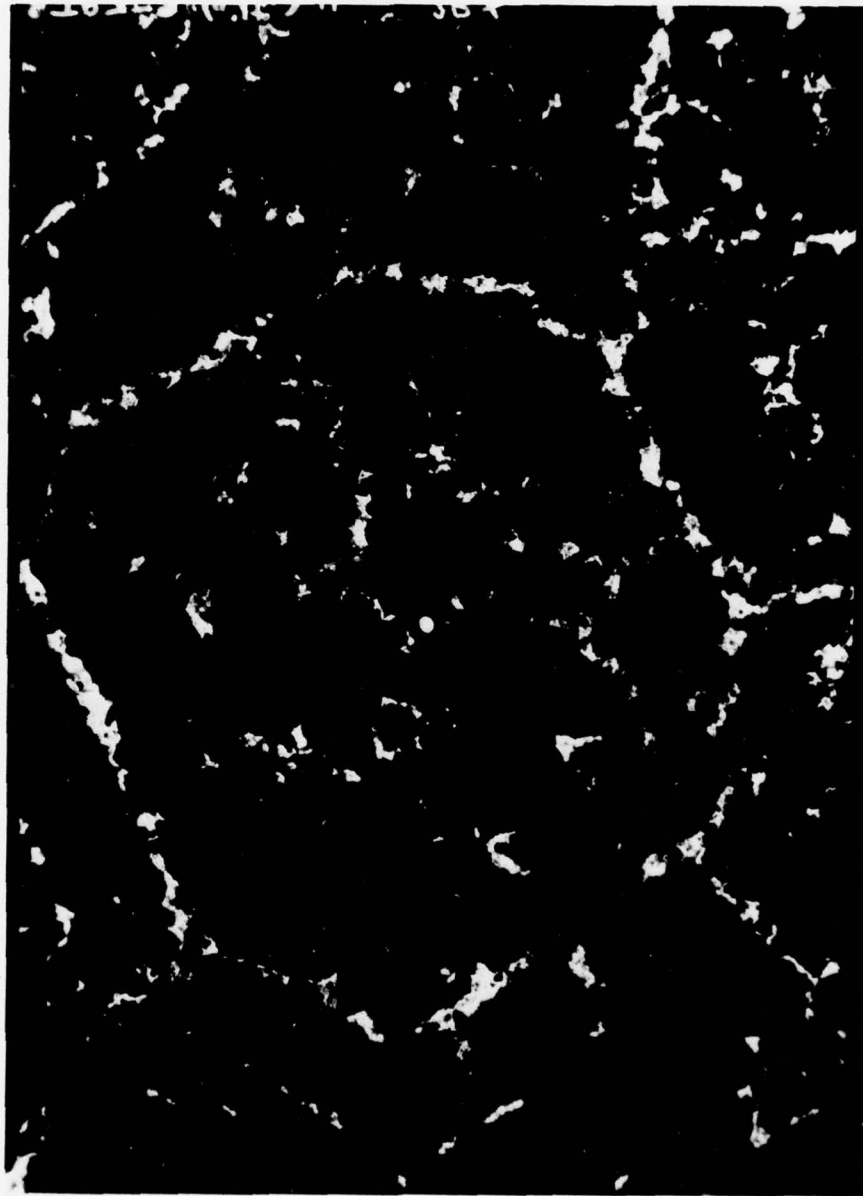
Figure 38. Magnification of 28× of a horizontal thin section
of the Toledo Penn 7 material after freezing

PART III: EVALUATION

54. In order to assess the potential of enhancing consolidation of
dredged material by freezing in the field, it was necessary to extrap-
olate and combine the laboratory data with estimates of other factors
that would affect freezing and drainage in disposal areas. The most im-
portant factors were climate, especially temperature and snowfall, and
site management, including snow removal and freezing as well as drainage
enhancement techniques. A well-designed and monitored field demonstra-
tion project is probably the only satisfactory way of evaluating the
overall potential of the freeze-thaw enhancement technique.

Depth of Frost Penetration

55. The depth of frost penetration expected at a particular dis-
posal site is a function of several properties of the dredged material
and the climatological properties at the site. It can be predicted
using the modified Berggren equation (Office, Chief of Engineers, 1966),
which is expressed as

$$X = \lambda \sqrt{\frac{48 \ K \ nF}{L}} \tag{2}$$

where

X = depth of freeze (ft)*

λ = coefficient that takes into account the mean annual site
temperature T , the surface freezing index nF , the length
of the freezing season, the volumetric latent heat of fusion,
and volumetric heat capacity of the soil, $^{\circ}C$.

K = thermal conductivity of soil (Btu ft/hr ft^2 $^{\circ}F$)

n = conversion factor for air index to surface index

F = air freezing index ($^{\circ}F$-days)

L = volumetric latent heat of fusion (Btu/ft^3)

---

* A table of factors for converting U. S. customary units of measure-
ment to metric (SI) can be found on page 7.

56. For disposal sites in the area of the Great Lakes, λ generally varies between 0.7 and 0.85. A representative value of 0.75 was chosen to simplify Equation 2. Thermal conductivity K can be expressed (Kersten 1949) as

$$K = (0.033 \, \ln w - 0.017) \exp^{0.023\gamma_d} \tag{3}$$

where

w = water content (%)

γ_d = dry unit weight (lb/ft^3)

57. In turn, if the dredged material is assumed to be saturated, γ_d can be expressed as a function of water content and specific gravity of the soil solids G_s by

$$\gamma_d = \frac{\gamma_w}{\dfrac{1}{G_s} + \dfrac{w}{100}} \tag{4}$$

where γ_w is the unit weight of water (lb/ft^3). The volumetric latent heat of fusion L is given (Office, Chief of Engineers, 1966) as

$$L = \frac{144 \, \gamma_d w}{100} \tag{5}$$

58. Assuming a value of 1.0 for the conversion factor in Equations 3 and 5 can be used to simplify Equation 2 yields an expression for frost depth as a function of dry unit weight, water content, and freezing index:

$$X = 137 \left[\frac{(0.033 \, \ln w - 0.017) \exp^{0.023\gamma_d}}{\gamma_d w} \right]^{1/2} \left(\frac{F}{1000} \right)^{1/2} \tag{6}$$

59. Equations 4 and 6 were used to construct a plot, shown in Figure 39, of frost depth as a function of water content and freezing index. A representative specific gravity of 2.63 was used in Equation 4. Water content had little effect on freeze depth for water contents in excess of 75 percent. However, freeze depth increased dramatically with

48
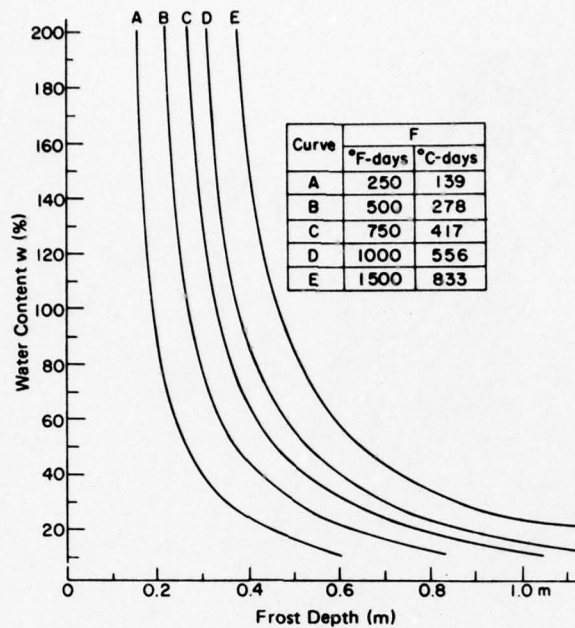
Figure 39. Depth of freeze as a function
of water content and freezing index

decreasing water content at water contents less that 35 percent.

60. Mean annual freezing index can be estimated from the contour map shown in Figure 40, or for a particular site, it can be calculated from U. S. Weather Service published data. Such calculations are shown in Figure 41 for six cities situated on the Great Lakes with dredged material disposal sites. Mean monthly temperature is plotted. Freezing index is estimated by calculating the area between the freezing line, 32°F, and the mean air temperature curve. The mean freezing index ranged from a low of 270 °F-days at Cleveland to a high of 1226 °F-days at Green Bay. The calculated freezing indices are compared with those estimated from the contour map in Table 3. Generally, those from the map tend to be higher than the corresponding calculations, with considerable discrepancies for Cleveland, Toledo, Detroit, and Chicago.

61. Anticipated mean freezing depths for disposal sites at the six cities are also included in Table 3. These were obtained from Figure 40 using the calculated freezing indices and a water content of 60 percent, which is representative of the disposal sites in these areas.

49

Mean air freezing index values
are cumulative degree days below 32°F, computed
on basis of mean air temperature data.

The isolines of mean air freezing index were drawn
using data from the 361 U.S. Weather Bureau Stations shown
as dots on the map. The map is offered as a guide only. It does not
attempt to show local variations, which may be considerable, particularly
in mountainous areas.

The actual mean air freezing index used should be computed for the
specific project using temperature data from station nearest site.

Freezing index in degree days below 0°C can be computed by multiplying by 5/9.

Figure 40.   Distribution of mean air freezing indices in the continental U. S.
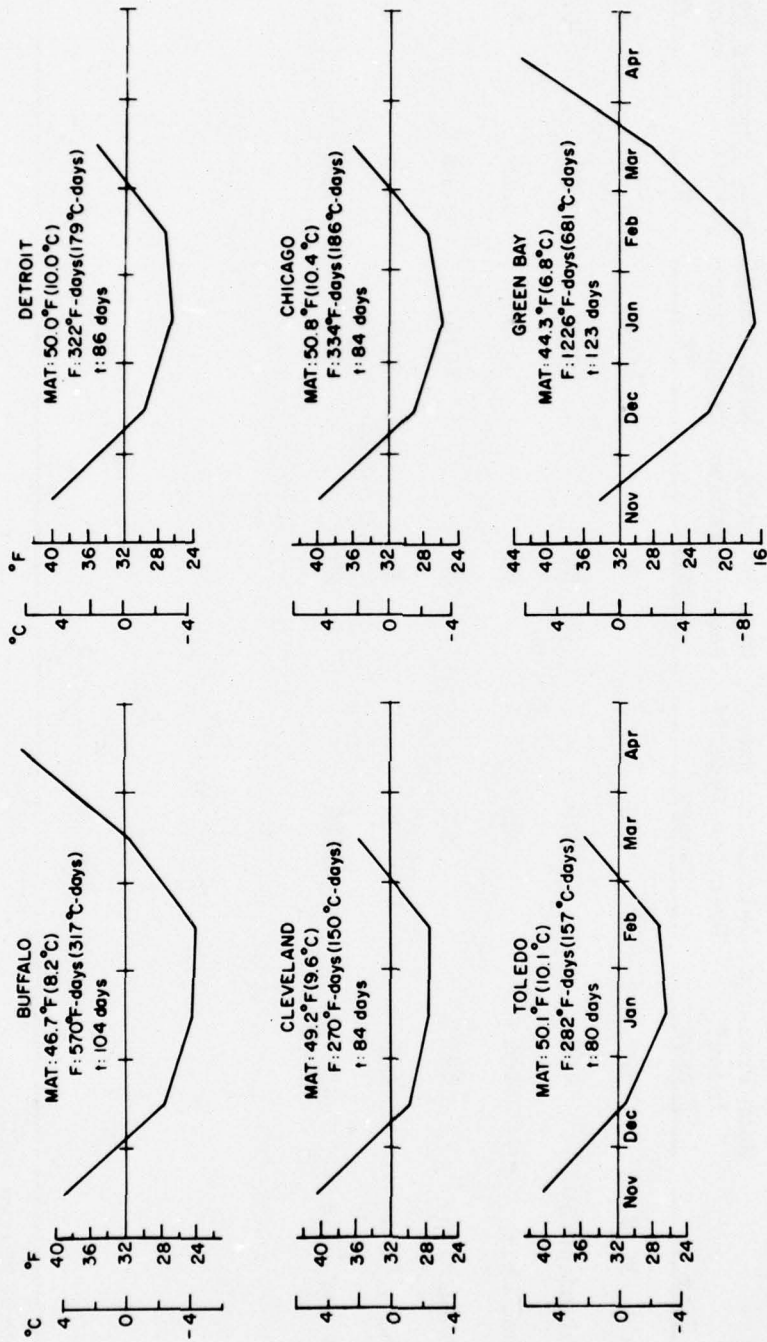
Figure 41. Computation of freezing index at six cities along the Great Lakes

Table 3

Summary of Climatological Data from Six Great Lakes Cities

and Predicted Depth of Frost Penetration

Site	Mean Freezing Index* °F-days	Calculated Mean Freezing Index** °F-days	Mean Freezing Season Duration Days	Mean Annual Temperature °F	Anticipated Mean Freezing Depth w=60%† m	w=40%†† m
Buffalo, N. Y.	525	570	104	46.7	0.24	0.30
Cleveland, Ohio	400	270	84	49.2	0.16	0.20
Toledo, Ohio	400	282	80	50.1	0.16	0.20
Detroit, Mich.	625	322	86	50.0	0.18	0.24
Chicago, Ill.	625	334	84	50.8	0.18	0.24
Green Bay, Wis.	1300	1226	123	44.3	0.37	0.45

* From Figure 40.
** From U. S. Weather Service data.
† Assumes all water freezes.
†† Assumes 20 percent unfrozen water content.

52

Anticipated freeze depths ranged from 0.16 m at Cleveland to 0.37 m at Green Bay.

62. The anticipated freeze depths may be greater than calculated using the total water content of the dredged material, since large amounts of unfrozen water in fine-grained f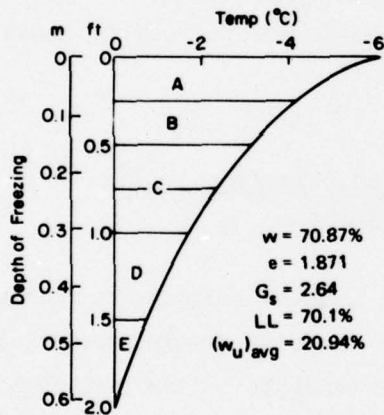rozen material were not accounted for in the equations used to plot Figure 39. Unfrozen water content tests were not conducted on the dredged material because the facilities at CRREL were not in operation; however, estimates of the unfrozen water contents of typical fine-grained materials were made from the liquid limits.

63. Figure 42 illustrates the unfrozen water content w_u as a function of liquid limit and temperature as reported by Tice et al. (1976). It can be

Figure 42. Unfrozen water content vs liquid limit

seen that for materials with high liquid limits, the unfrozen water content can be very significant. If the temperature with depth profile is assumed as in Figure 43, the average unfrozen water content over the full depth would be estimated to be 21 percent of 70.1 percent.

64. However, since the frost depth is relatively insensitive to water content at the water contents

Increment	T_{avg}	w_u (%)	w_f (%)	V (%)
A	-4.9	14.0	56.87	12.50
B	-3.6	15.5	55.37	12.50
C	-2.35	17.5	53.37	25.00
D	-1.2	21.5	49.37	25.00
E	-0.35	30.0	40.87	25.00

Figure 43. Assumed temperature profile

53

of interest, only a small increase in expected frost penetration results. Expected frost penetrations assuming 20 percent unfrozen water are also included in Table 3. The Green Bay figure of 0.45 m agrees well with a measured depth of 0.6 m $\pm$ 0.15 m taken at the Bayport disposal area on 1 March 1976.

65. The presence of significant amounts of snow will inhibit frost penetration. Snow cover acts as an insulating blanket by slowing the heat flow from the relatively warm dredged material to the relatively cold air. Mean snowfalls for the six cities are plotted in Figure 44. Annual snowfall ranges from a high of 2.24 m at Buffalo to a low of 0.79 m at Toledo. Cities lying to the west of the lakes have a mean annual snowfall of 1.0 m or less. In a normal year this amount of snow distributed over a winter season may have little effect on frost pene-tration. As of 1 March 1976, Cleveland, Toledo, Detroit, and Chicago had no snow on the ground, and Green Bay had only 0.1 m and Buffalo a trace. However, snow in the Buffalo area would be expected to signifi-cantly decrease the depth of freezing, especially in a year of heavy snowfall (3.5 m being not uncommon).

Potential Benefits of Enhanced Consolidation and Increased Permeability

66. Both thaw-enhanced consolidation and the subsequent increase in permeability can be of value in rapidly reducing dredged material volume. In order to explore the potential benefits of the two phenomena, laboratory data have been extrapolated to field situations. Data from the Toledo Island site were chosen as representative and were used in the extrapolations. As is usually done in consolidation studies, the problem was broken down into two components; the ultimate consolidation was separated from the rate effects. Thus, the first part of this analysis considers only the ultimate settlements achievable, without regard for the time required to obtain them, while the second part concentrates on the settlements as they relate to time.
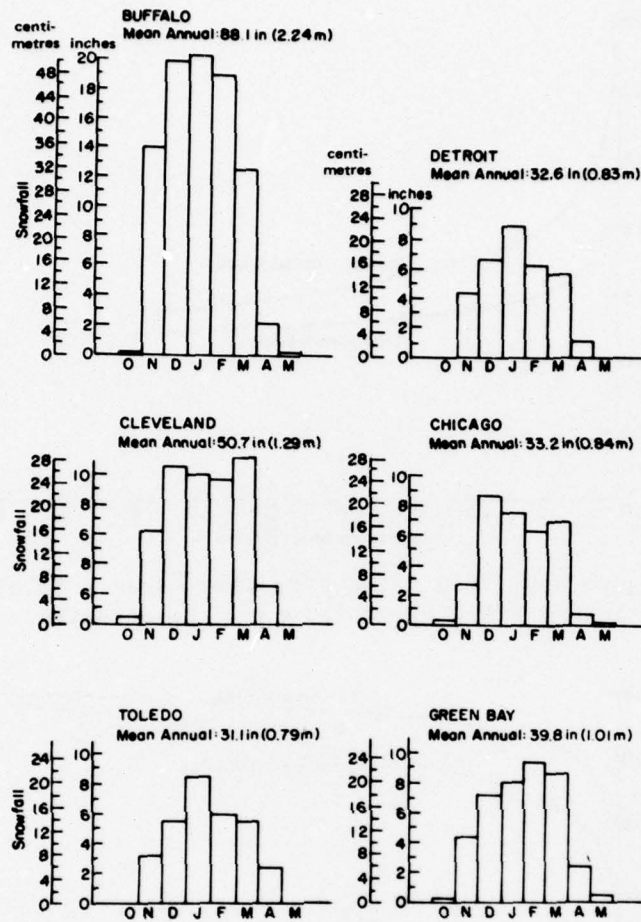
Figure 44. Mean snowfall in six cities along the
Great Lakes

Settlement

67. The void ratio-effective stress data from the Toledo Island
site have been replotted on a linear scale in Figure 45. Both nor-
mally consolidated and freeze-thaw consolidated (for one freeze-thaw
cycle) curves are shown. Void ratio is converted to dry density and
plotted as a function of effective stress in Figure 46 using the
relationship:

$$\gamma_d = \frac{G_s}{e + 1} \tag{7}$$

55
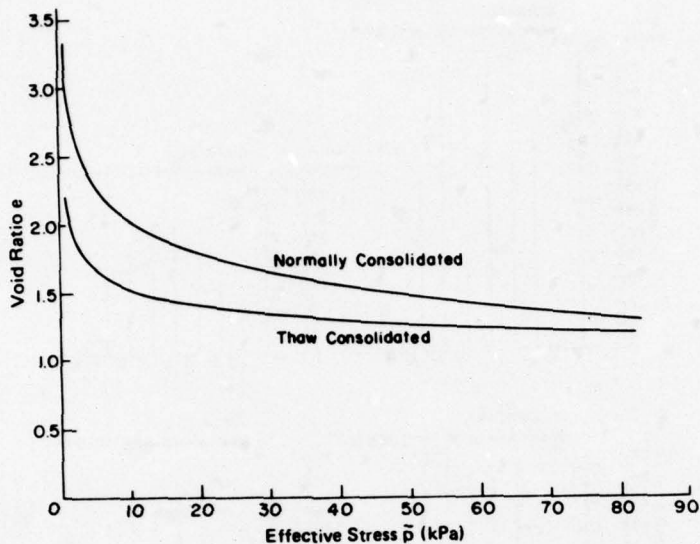
Figure 45.   Void ratio-effective stress, Toledo
Island site, replotted on a linear scale

Figure 46.   Dry density vs effective stress,
Toledo Island site

where the specific gravity of solids is, in this case, 2.63. Both the
normally and thaw-consolidated curves are shown.

Initial state

    68.   In order to utilize these data, assumptions regarding the ini-
tial state of the dredged material must be made. According to Johnson
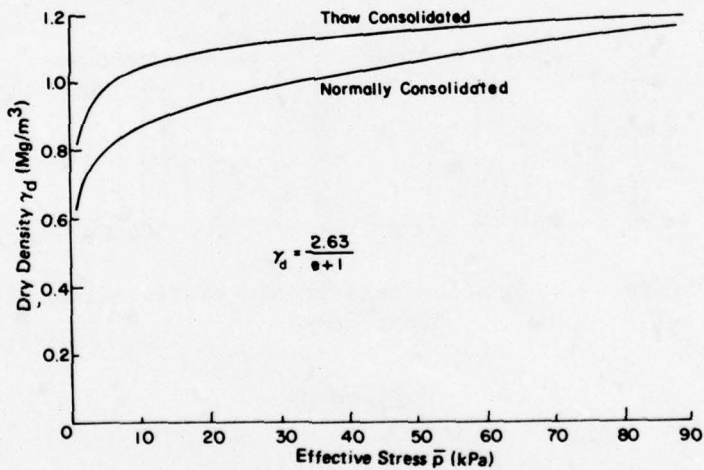
56

et al. (1977), the water content immediately after sedimentation may be
several times greater than the liquid limit. It decreases rapidly
through surface drainage to between 1.0 and 1.5 times the liquid limit.
These figures are in general agreement with the findings of this study
which showed water contents approximately equal to the liquid limit for
most of the samples obtained (Figure 17). Accordingly, an initial water
content of 80 percent was chosen for the Toledo Island material, which
is approximately 1.1 times its liquid limit. A specific gravity of
solids equal to 2.63 corresponds to a dry density of 0.85 Mg/m^3. The
representative site was assumed to have a constant initial dry density
γ_{di} and water content over all depths. In accordance with Terzaghi's
consolidation theory (Terzaghi and Peck 1966), the pore water was as-
sumed to carry all stress initially, and, upon completion of consolida-
tion and dissipation of excess pore pressure, the mineral structure was
assumed to carry all stress. If a material were allowed to consolidate
under its own weight, the ultimate effective stress on the soil skeleton
at any depth Z would be the buoyant unit weight of soil γ_b multi-
plied by the depth:

$$\bar{p} = \gamma_b Z \tag{8}$$

69. To facilitate the computations, ultimate stresses were assumed
to develop without the corresponding volume reduction that would nor-
mally occur. In turn, for a given depth, volume strain could be calcu-
lated and the total settlement computed by integrating the strain over
depth (all strains were assumed to be one-dimensional). The ultimate
effective stress was plotted as a function of depth in Figure 47.

70. Buoyant unit weight was taken as 0.527 Mg/m^3 and Equation 3
reduced to

$$\bar{p} = 5.168Z \tag{9}$$

where Z is in metres and $\bar{p}$ in kilopascals.

71. The effective stress plot from Figure 47 can be combined with the normally consolidated dry density curve from Figure 46 to produce a plot of dry density as a function of depth due to gravitational loading as shown in Figure 48. The initial dry density of 0.85 Mg/m^3 is depicted, along with the final dry density γ_{df} resulting from gravity. Final dry density at any depth is obtained by taking the effective stress at that depth from Figure 47 and reading the dry density at that effective stress from the normally consolidated curve in Figure 46. For depths less than 1.4 m, the effective stress was not sufficient to produce dry densities in excess of the initial assumed density of 0.85 Mg/m^3, so that initial conditions were unchanged above this depth.

Gravitational consideration

72. Three comparisons to the gravitational consolidation curve are shown in Figure 48. However, before discussing these comparisons, it should be noted that, following freeze-thaw consolidation, gravitational consolidation is still assumed to take place. This would occur
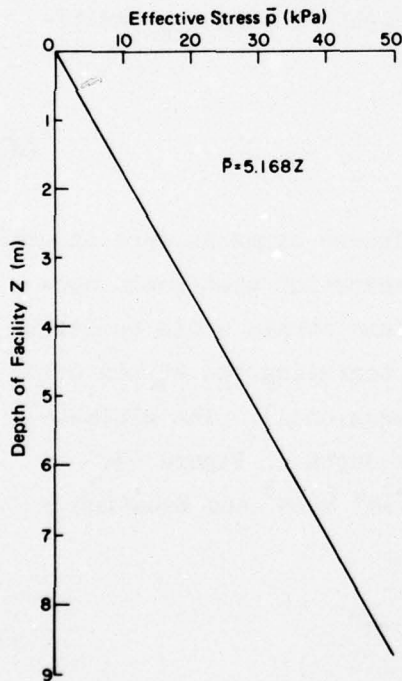
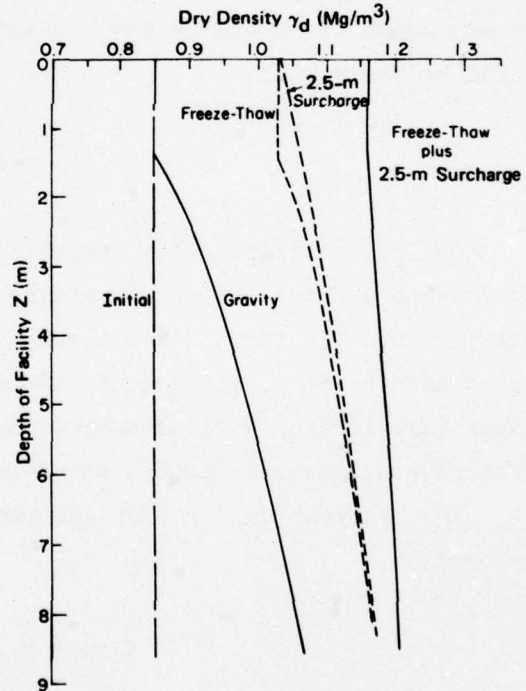Figure 47. Ultimate effective stress vs depth

Figure 48. Dry density vs depth

during the warm season and would be speeded considerably by the increased permeability resulting from the freeze-thaw cycle. Also the entire depth of material is considered to have undergone freezing and drainage subsequent to thawing. In practice, this could only be accomplished over a number of winter seasons, limiting the lift thickness of new material deposited each summer to a depth that could be completely frozen the following winter.

73. The first comparison with the gravitation consolidation curve is the expected ultimate dry density after a single freeze-thaw cycle. Initial conditions were assumed equal in all instances (i.e., 0.85 Mg/m^3 over all depths). The freeze-thaw density relationship was obtained in the same manner as the gravitational curve, except that the thawed data from Figure 46 were used in place of the normally consolidated data. Again, above a depth of 1.4 m, gravity did not contribute to the consolidation. Below this depth additional consolidation would occur due to gravity, with the effective stress being equal to that used in the normally consolidated case.

74. The second comparison shown in Figure 48 is with the anticipated dry density that would ultimately result by adding a 2.5-m-thick surcharge of a material of 1.6 Mg/m^3 density to the dredged material. Assuming the entire surcharge would act above the water table, the effective stress depicted in Figure 47 would be increased by a constant value equal to the unit weight of the surcharge multiplied by the depth of the surcharge. In this case the effective stress (in kilopascals) as a function of depth is

$$\overline{p} = 5.168Z + 39.325 \qquad (10)$$

Using the effective stress given in Equation 10, dry density as a function of depth is obtained from the normally consolidated curve in Figure 46.

75. The final comparison shown in Figure 48 is for the case in which dredged material undergoes one freeze-thaw cycle and is subsequently loaded by a 2.5-m-thick surcharge as above. Effective stress as

59

a function of depth is again obtained from Equation 10 and dry density
from the thawed curve in Figure 46.

Volumetric strain

76. The dry density relationships plotted in Figure 48 can be converted to ultimate volumetric strain ϵ_v using the equation:

$$\epsilon_v = -\left(1 - \frac{\gamma_{di}}{\gamma_{df}}\right) 100\% \tag{11}$$

where volumetric strain is a percentage. Volumetric strain as a function of depth is plotted in Figure 49 for each case shown in Figure 48.

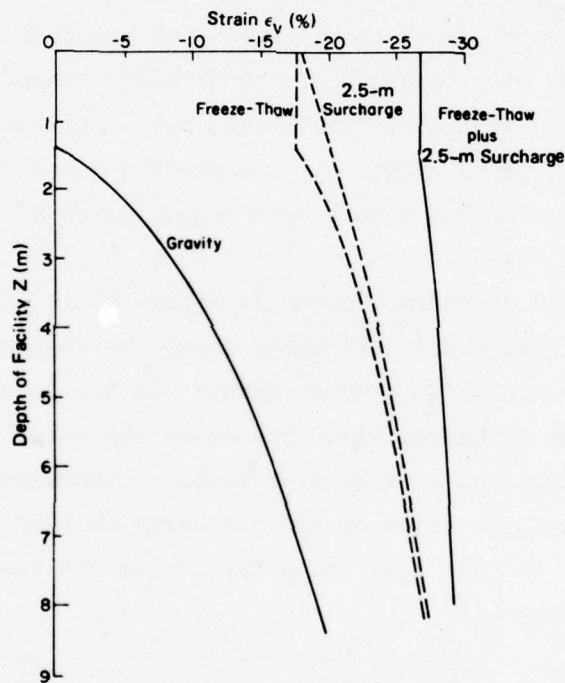Figure 49. Volumetric strain as a
function of depth

Since one-dimensional consolidation is assumed, integrating the volumetric strain with respect to depth yields the expected ultimate settlement as a function of depth. Integrations for each of the four cases are shown in the plot of total ultimate settlement as a function of the original depth of the dredged material in Figure 50. It is apparent

60
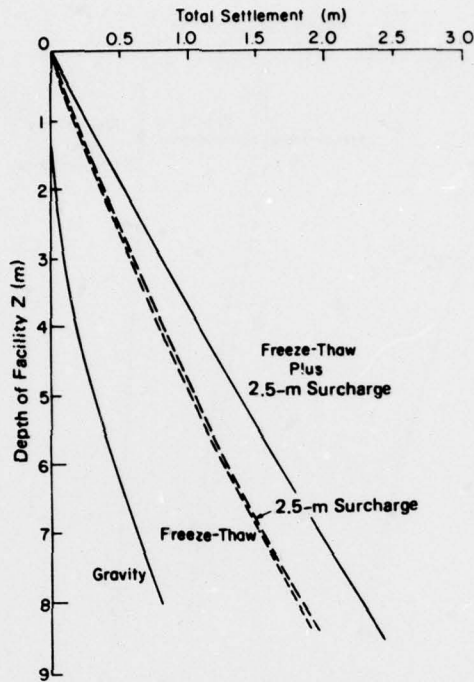
Figure 50. Total ultimate
settlement as a function of
original depth

that the consolidation resulting from one freeze-thaw cycle is equiva-
lent to that produced by the 2.5-m-thick surcharge. An additional sig-
nificant volume reduction can be attained by applying the 2.5-m-thick
surcharge to the thaw-consolidated material.

Volume reduction

77. The settlement data from Figure 50 have been converted to
volume reduction percentages by dividing the settlement by the original
depth of material. These data are shown in the plot of volume reduction
as a function of original depth in Figure 51. Volume reduction for the
thaw-consolidated and surcharge-consolidated materials ranged from 18
percent for shallow facilities to 23 percent for an 8-m original mate-
rial depth. Addition of a 2.5-m-thick surcharge to the thaw-consolidated
material results in a total volume reduction of approximately 27 percent.
The influence of gravity is minor in this case.

61
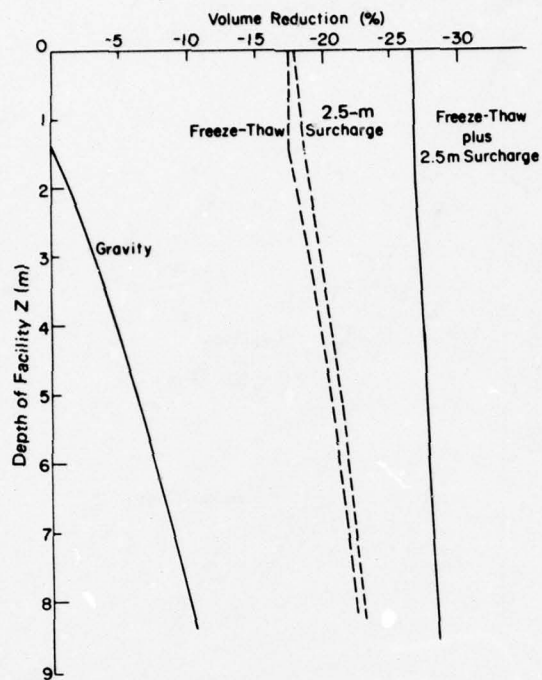
Figure 51. Volume reduction as a
function of original depth

Secondary consolidation

78. It should also be pointed out that secondary consolidation has
been ignored in this analysis. In general, the tests showed very little
secondary consolidation. Only at very low effective stresses was there
consequential secondary consolidation. It is felt that this would have
very little effect on the overall volume reductions resulting from
either thaw or surcharge consolidation.

Rate Effects

79. Taylor (1948) in his discussion of Terzaghi's consolidation
theory showed that the rate of pore pressure dissipation is proportional
to the coefficient of consolidation c_v , which can be expressed as

$$c_v = \frac{k(1 + e)}{a_v \gamma_w} \tag{12}$$

62

where a_v is the coefficient of compressibility. Permeability for both the thaw-consolidated and normally consolidated Toledo Island materials is given in Figure 28 as a function of void ratio. The coefficient of compressibility is defined as

$$a_v = - \frac{de}{dp} \qquad (13)$$

which is the negative of the slope of the void ratio-effective stress curves shown in Figure 45. The coefficient of compressibility is plotted as a function of void ratio in Figure 52. The permeability and

compressibility curves from Figures 28 and 52 can be combined according to Equation 12 to produce the coefficient of consolidation as a function of void ratio. This is plotted for both the thawed and normally consolidated cases in Figure 53. Using the void ratio-effective stress plots of Figure 45, the coefficient of consolidation can be more conveniently expressed as a function of effective stress as shown in Figure 54.

80. The preceding two figures (53 and 54) demonstrate that the coefficient of

Figure 52. Coefficient of compressibility as a function of void ratio

consolidation can be an order of magnitude or higher for the thaw-consolidated material than for the normally consolidated. This is principally due to the tremendous increase in permeability resulting from the freeze-thaw consolidation. The coefficient of consolidation is relatively constant with respect to effective stress for the normally consolidated material but varies greatly for the thaw-consolidated
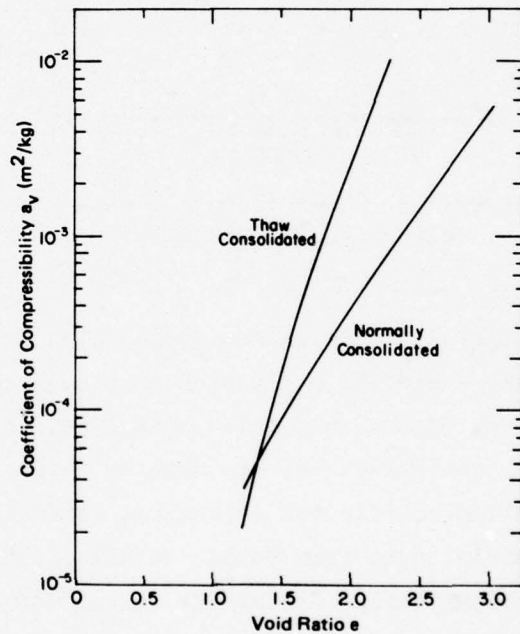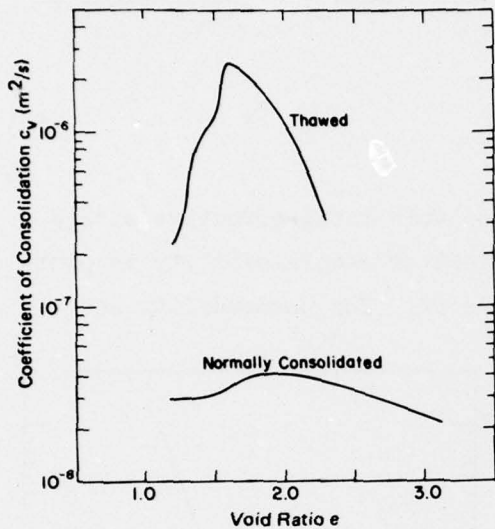
63

Figure 53. Coefficient of con-
solidation vs void ratio
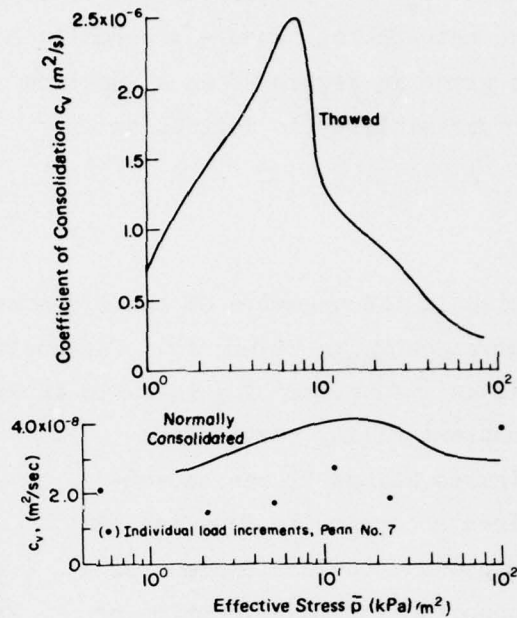
Figure 54. Coefficient of consol-
idation as a function of effective
stress

material. This large variation is typical of published data and would
make a precise evaluation of time-dependent consolidation difficult. A
check of the calculated consolidation coefficient for the normally con-
solidated material was made by comparing it with values of the consoli-
dation coefficient determined directly from laboratory tests. Unfortu-
nately, data from Toledo Island could not be used because drainage con-
ditions varied during the tests; data from the Penn 7 area, a nearby
site containing similar material, were used instead. Measured values of
c_v the consolidation coefficient for five different mean effective
stresses are plotted in Figure 54 along with the calculated value. They
were obtained using the square root of time fitting method outlined in
Taylor (1948). The overall agreement is good, with the measured coeffi-
cients ranging from about 1/2 to 2/3 the value of the calculated.

81. In order to get a rough estimate of the effect of the varia-
tion of the coefficients of consolidation for the thawed and normally
consolidated materials on the overall time required to consolidate

64

dredged material in the field, a simple comparison was made. A constant coefficient of consolidation of 2.0×10^{-8} m^2/s for the normally consolidated material and a constant of 1.0×10^{-6} m^2/s for the thawed material were selected and assumed independent of load. This assumption will, of course, give only a crude approximation of the consolidation rate in the thawed material. The consolidation time t is given by Terzaghi and Peck (1966) as

$$t = \frac{T_v H^2}{c_v} \tag{14}$$

where T_v is the longest possible drainage path and H is a time factor related to the degree of consolidation U under consideration. Assuming a 90 percent degree of consolidation to be desirable, the time factor is found to be approximately 0.9 from Terzaghi and Peck (1962). No bottom drainage is assumed; thus the longest possible drainage path equals the thickness of the dredged material in all cases. Consolidation times computed from Equation 14 are plotted as a function of depth in Figure 55.

82. The consolidation times are independent of applied load as the consolidation coefficient was assumed independent of load. It can be seen that for a layer 1 m thick, 0.028 yr (10 days) is required to reach 90 percent consolidation for the thaw-consolidated case, while 1.41 yr is required for the normally consolidated case, a difference factor of 50. Similarly, for a 2-mm-thick layer the
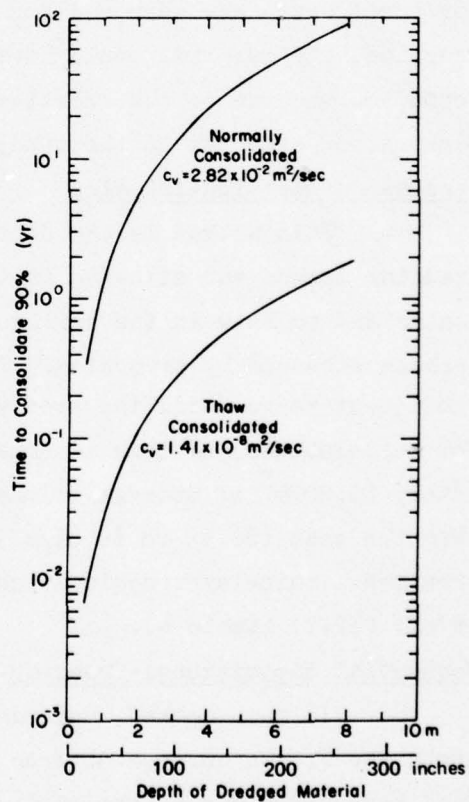

Figure 55. Time to 90 percent consolidation vs depth

65

corresponding times become 0.11 yr (41 days) vs 5.64 yr. It is clear
that there is merit in taking advantage of the shorter consolidation
times for the thawed material.

Site Management

Freezing techniques

83. In making the comparison between the thaw-consolidated and con-
ventionally consolidated cases, the actual mechanics of freezing a dis-
posal site have been ignored. In order to conveniently compare equal
volumes of material, the hypothetical site was assumed to be filled to
capacity and subsequently frozen completely. In this way, the depth of
material at the initial assumed density and water content was identical
for the freeze-thaw case and for the gravity and surcharged cases. In
practice, the material would have to be frozen sequentially as it is
deposited because of the relatively shallow depths of seasonal frost
penetration expected at the study sites.

Seasonal deposition-freezing

84. This method is the depositing of a layer of material each
dredging season and allowing it to freeze completely during the winter
months and to thaw in the spring with underdrains or surface drainage,
perhaps enhanced by trenching. The process could be then repeated during
subsequent years until the area was filled. The cost (see Appendix A
for calculations) of this seasonal deposition-freezing would be approxi-
mately $0.20/m^3 of storage volume gained. This is considerably less
than the cost ($0.43 to $0.81/m^3) for the least expensive conventional
treatment, thin-layer desiccation and trenching, reported by Johnson
et al. (1977) (Table 4).

Sequential depositional-freezing

85. In this method, unfrozen dredged material is pumped from be-
neath the frozen surface or from an adjacent site onto the frozen sur-
face repeatedly during the winter, allowing each layer to freeze before
the next is applied. Each layer would be only 50 to 75 mm in thickness.
This would not necessarily increase the depth of freezing significantly

66

Table 4

Costs of Several Conventional Densification Treatments*

Treatment	Added Storage in Cubic Yards Per Acre for LL of				Cost Densification Treatment - Dollars Per Cubic Yard				
					Per Cubic Yard of Storage for LL of				Per Acre of Disposal Area
	50	100	150	200	50	100	150	200	
Desiccation-placing in thin layers; draining and trenching	2580	3870	4520	4840	0.62	0.42	0.36	0.33	1,600
Underdrainage layer with collectors, no membrane, ponded water surcharge, and no pumping, seepage consolidation	1200	1900	2210	2360	2.30	1.50	1.30	1.20	2,800
Underdrainage, with sand blanket and collectors	600	940	1100	1160	4.70	3.00	2.60	2.40	2,800
Underdrainage layer with collectors; vacuum induced by pumping	1190	1850	2150	2300	6.10	3.90	3.40	3.20	10,100
5-ft-high temporary surcharge fill	1180	1860	2150	2290	6.80	4.40	3.80	3.50	8,100
16-ft-deep water ponded with membrane, sand blanket, and collectors	1740	2730	3160	3390	7.30	4.60	4.00	3.70	12,700
10-ft-high temporary surcharge fill	1740	2730	3160	3390	9.30	5.90	5.10	4.80	16,100
8-ft-deep water ponding with membrane, sand blanket, and collectors	1180	1860	2150	2290	10.80	6.80	5.40	5.50	12,700

* From Johnson et al. (1977).

67

as the bottom of the frozen material might thaw. However, it would increase the quantity of material frozen during a given winter.

86. It is assumed that the improved permeability and consolidation properties of the thawed material beneath the frozen material would not change significantly with time, as this material could not consolidate until the frozen material thawed completely and surface drainage was available. Delaying the application of the load on the Penn 7 material for 54 days resulted in no significant difference in the degree of thaw consolidation (Figure 25).

Operating costs

87. The cost of operating pumps would add another $0.87/m^3 to the costs of managing the disposal site but would be advantageous because of the increased volume of material treated (calculations for pumping costs are given in Appendix A).

88. Snow removal could also add additional operational costs, especially in areas of high snowfall such as Buffalo. This problem would be particularly difficult until sufficient depth of frost was achieved to support heavy equipment. If a heavy snow cover accumulated before sufficient frost penetration was achieved, it would probably not be possible to remove the snow, and the disposal area would not freeze significantly. The costs of simply moving the snow to the sides with a road grader are estimated in Appendix A. For high snowfall areas such as Buffalo, the cost of snow removal is estimated to be approximately $0.46/m^3 of storage capacity achieved for the sequential deposition and freezing case.

89. The economics of managing a dredged material disposal site are presented in Table 5 for two methods: (1) seasonal deposition and freezing with trenching and (2) sequential deposition and freezing with trenching. Both methods assume that the snow will be removed mechanically. The volume of storage gained and the cost are presented for six cities in the Great Lakes region in Table 5. The costs of the first method vary considerably with the amount of seasonal snowfall and frost depth, being the greatest in Buffalo, $1.31/m^3, and smallest in Green Bay, $0.66/m^3.

Table 5

Additional Storage Volume and Estimated Costs

for Two Freezing Treatments

	Buffalo	Detroit	Toledo	Cleveland	Chicago	Green Bay
Depth of frost penetration, m*	0.46	0.37	0.30	0.30	0.37	0.55
Seasonal snowfall, m**	2.24	0.83	0.79	1.29	0.84	1.01
Length of freezing season, days†	104	86	80	84	84	123
No. of 150-mm snowfalls removed††	8	3	3	5	3	4
Freezing treatment						
Seasonal deposition and freezing with trenching:						
Vol of storage gained, m^3/m^2‡	0.072	0.058	0.047	0.047	0.058	0.087
Cost of trenching, $/m^3$‡‡	0.20	0.20	0.20	0.20	0.20	0.20
Cost of snow removal, $/m^3$‡‡	1.11	0.52	0.64	1.06	0.52	0.46
Total Cost, $/m^3$	1.31	0.72	0.84	1.26	0.72	0.66
Sequential deposition and freezing with trenching:						
Depth of material frozen, m§	1.11	0.92	0.86	0.90	0.90	1.32
Vol. of storage gained, m^3/m^2‡	0.175	0.145	0.135	0.142	0.142	0.208
Cost of pumping, $/m^3$‡‡	0.87	0.87	0.87	0.87	0.87	0.87
Cost of trenching, $/m^3$‡‡	0.19	0.19	0.20	0.20	0.20	0.19
Cost of snow removal, $/m^3$‡‡	0.46	0.21	0.22	0.35	0.21	0.19
Total Cost, $/m^3$	1.52	1.27	1.29	1.42	1.28	1.25

* From Table 3.
** From Figure 44.
† From Figure 41.
†† Assumes 50% of snow melts.
‡ Assumes a thaw strain of 17.5% and a degree of consolidation of 90%.
‡‡ See Appendix A.
§ Assumes 75 mm of material frozen in a 7-day week during freezing season.

90. The second method, that of sequentially depositing and freezing during a single season, is more costly for all areas; however, a gain in storage volume of 2-1/2 to 3 times is made over the seasonal deposition method.

91. The cost of the sequential method could be reduced by eliminating the snow removal and assuming that all snow cover will be melted by the pumping of the dredged material on the frozen surface. This method would probably be effective in all the areas with the exception of Buffalo and would eliminate the problem of getting heavy equipment safely onto the frozen dredged material.

PART IV: DISCUSSION AND CONCLUSIONS

92. From the laboratory results, it can be concluded that freezing and thawing can be an effective means of enhancing the densification of fine-grained dredged material. As much as 20 percent or more volume reduction results (Figure 56) when dredged material with liquid limits
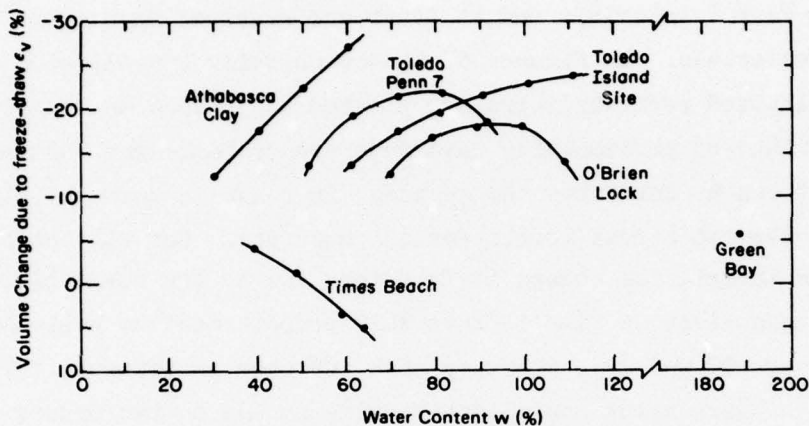

Figure 56. Volume change due to freeze-thaw vs water content for the five materials studied

in the range of 60 to 90 percent are subjected to one cycle of freezing and thawing. The degree of freeze-thaw consolidation enhancement appears to decrease with increasing amounts of coarse materials. For instance, the Times Beach material, which was the coarsest examined (Figure 17), underwent volume changes in the range of -4 to +5 percent, while the finer grained Toledo Island material changed from 13 to 24 percent. Likewise, plasticity is also a factor since the Green Bay material, with a grain-size distribution nearly the same as the O'Brien Lock material but a much higher plasticity index (138.4 vs 47.2), was reduced in volume by only 6 percent for the one test conducted vs 12 to 18 percent for the O'Brien Lock material. As the mineral types and chemical constituents were not identified, the contribution of these factors cannot be evaluated. Whatever the factors are that limit the degree of freeze-thaw consolidation enhancement, it appears that they are reflected in the values for the Atterberg limits, as the Times Beach material had the lowest liquid limit and plasticity index (38.9 and 9.3,

71

respectively) while the Green Bay material had the highest (198.0 and
138.4, respectively). Additional tests are required to establish the
relationships.

93. The vertical permeability of all the materials examined was
dramatically increased by freezing and thawing. This increase in per-
meability was as much as two orders of magnitude for the O'Brien Lock
and Toledo Penn 7 materials and at least one order of magnitude for all
the other materials. In Figures 57-61 the normally consolidated and
thaw-consolidated permeabilities are plotted as a function of void ratio
on a background of permeability data reported by Lambe and Whitman
(1969). It can be seen that the greatest increase in permeability oc-
curs at the lowest stress levels for all material. For all but the
Green Bay material, the change is from very low to low permeability.
Since the consolidation time is inversely proportional to permeability
(see Equations 12 and 14), the very high increase in permeability has
the effect of decreasing consolidation time by one to two orders of
magnitude for the materials examined. For the Penn 7 material, the re-
sult is to reduce the consolidation time for a layer 3 m thick from ap-
proximately 10 years to 3 months. From Figure 32 it can be seen that,
after thawing, the permeability falls with time. For the O'Brien Lock
material, the permeability before freeze-thaw was essentially recovered
after 25 days; however, a 21.5 percent reduction in volume had occurred.

94. The utility of freeze-thaw consolidation enhancement in field
situations is predicated on efficient use of natural freezing conditions
and on providing adequate drainage facilities. Field sites must be
managed to maximize the depth of frost penetration. This is especially
critical in the Great Lakes region because of the rather shallow 0.3
to 0.6 m of frost penetration that would normally occur. The depth of
freezing can be increased by sequentially placing and freezing shallow
lifts of dredged material during the winter. Trenching could be used to
improve surface drainage and snow could be removed to improve frost pene-
tration. The cost of such an operation is estimated to be in the range
of \$1.25 to \$1.52 m^3 of additional storage space obtained, which is com-
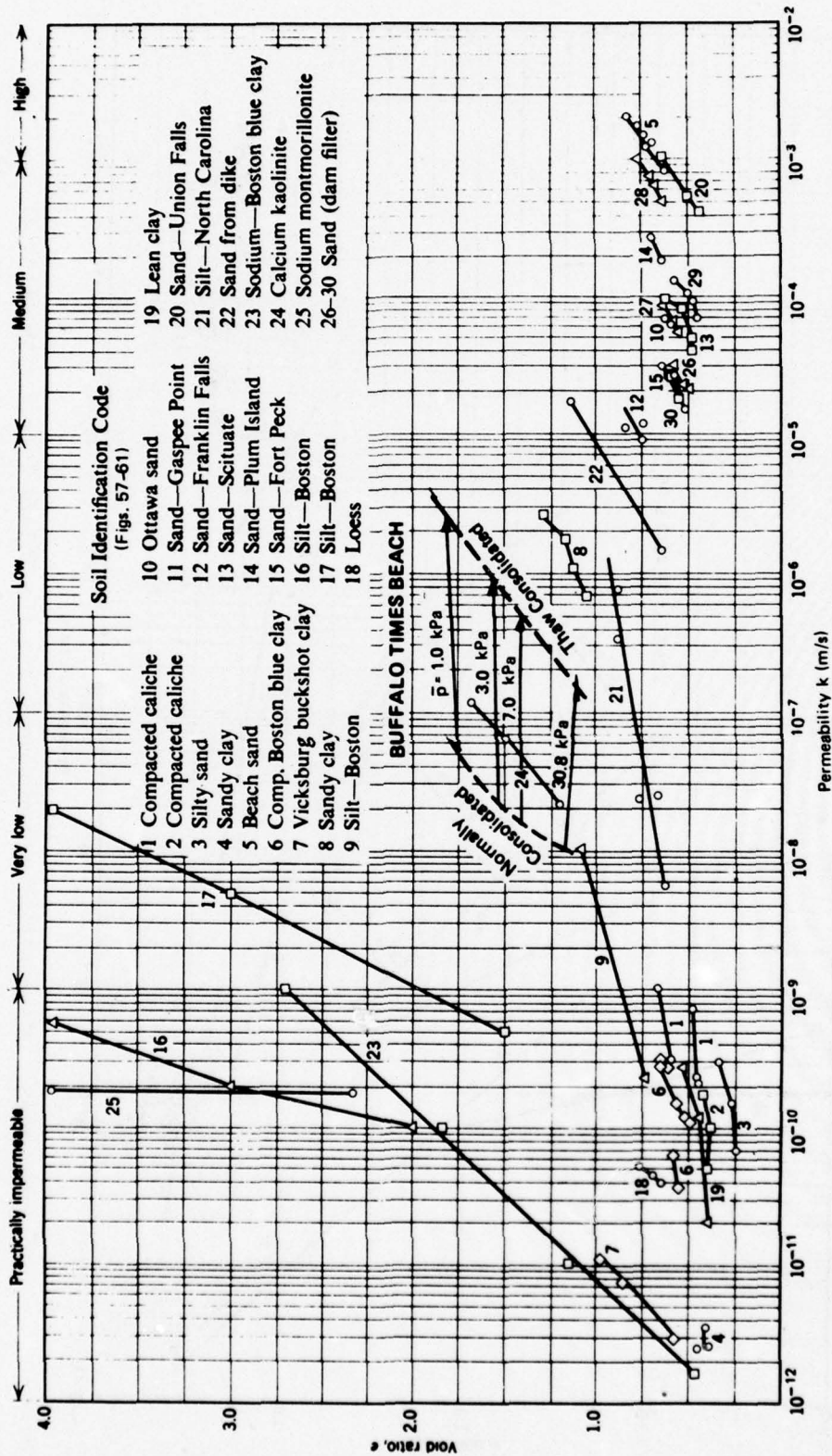petitive with such alternatives as placing shallow lifts and allowing

Figure 57. Permeability vs void ratio for the Buffalo Times Beach material
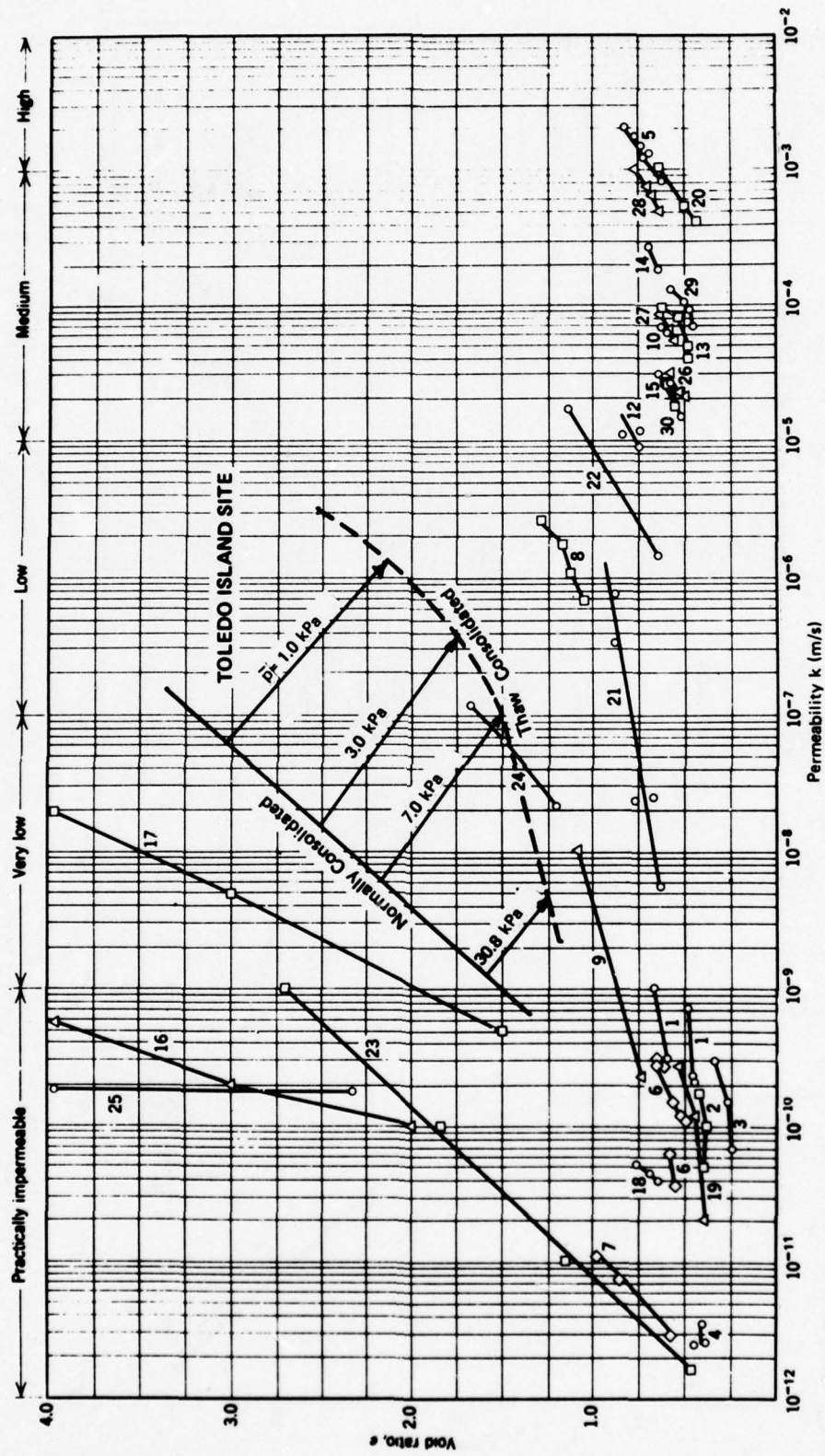
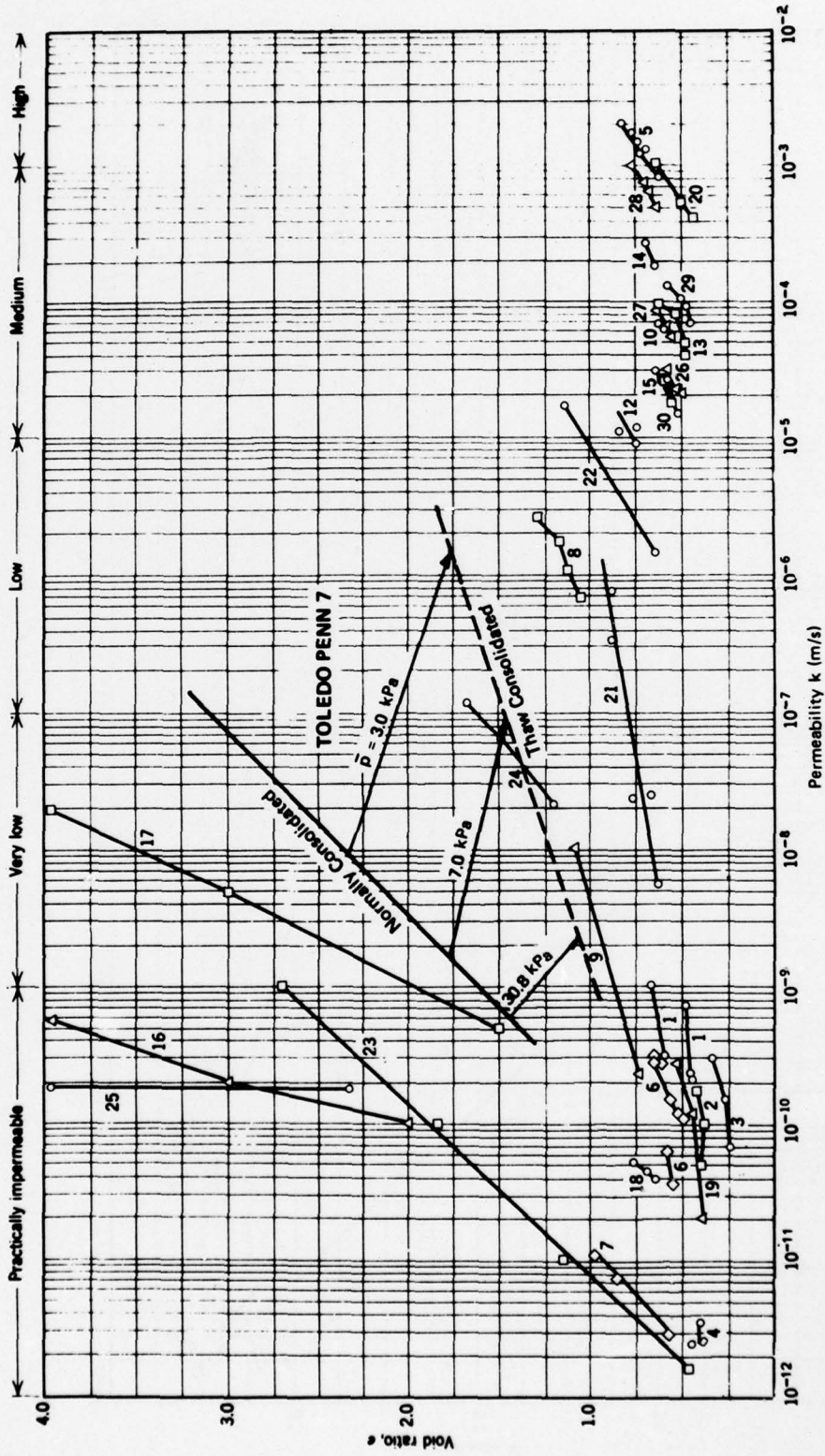Figure 58. Permeability vs void ratio for the Toledo Island site material

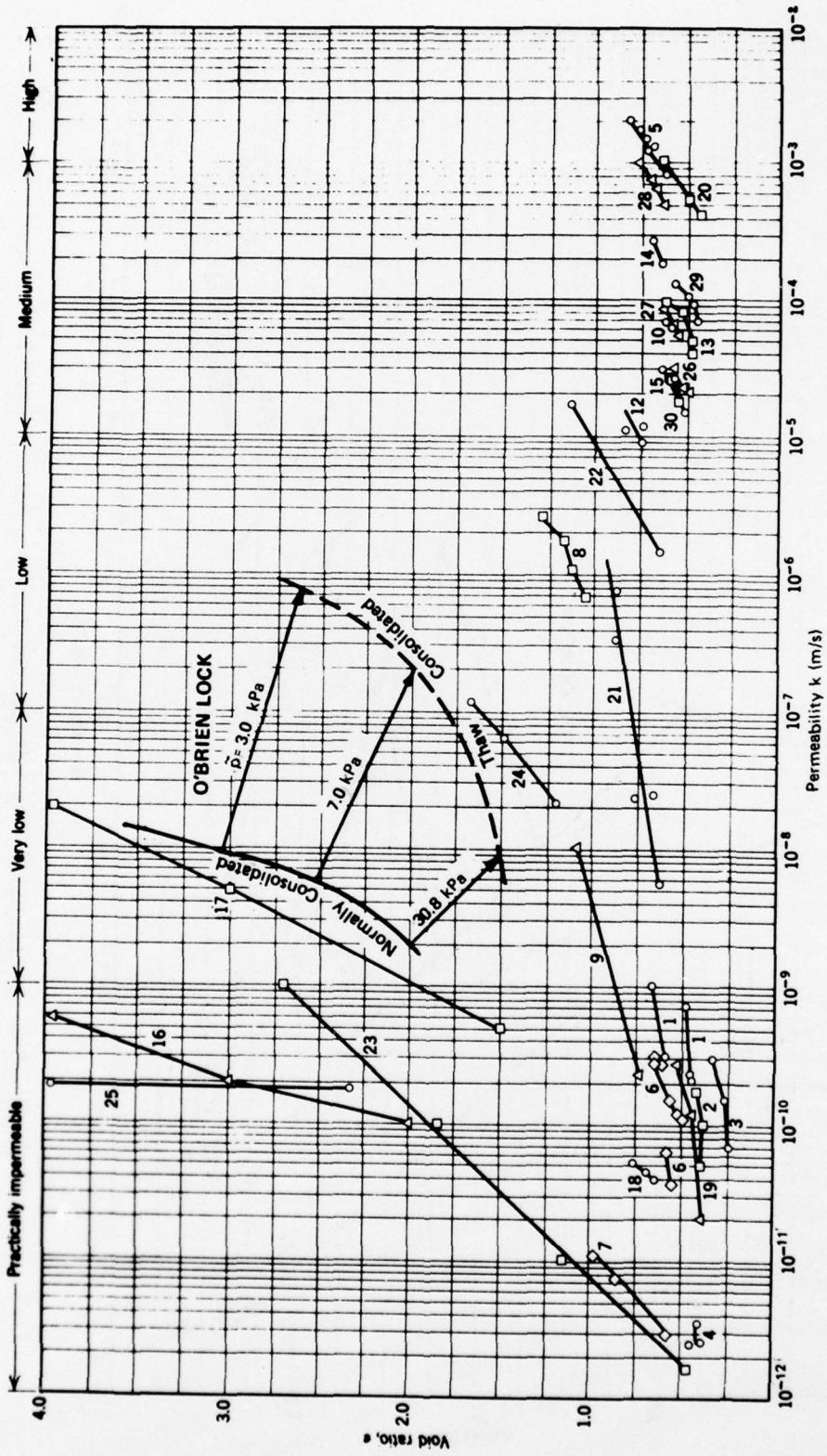Figure 59. Permeability vs void ratio for the Toledo Penn 7 material

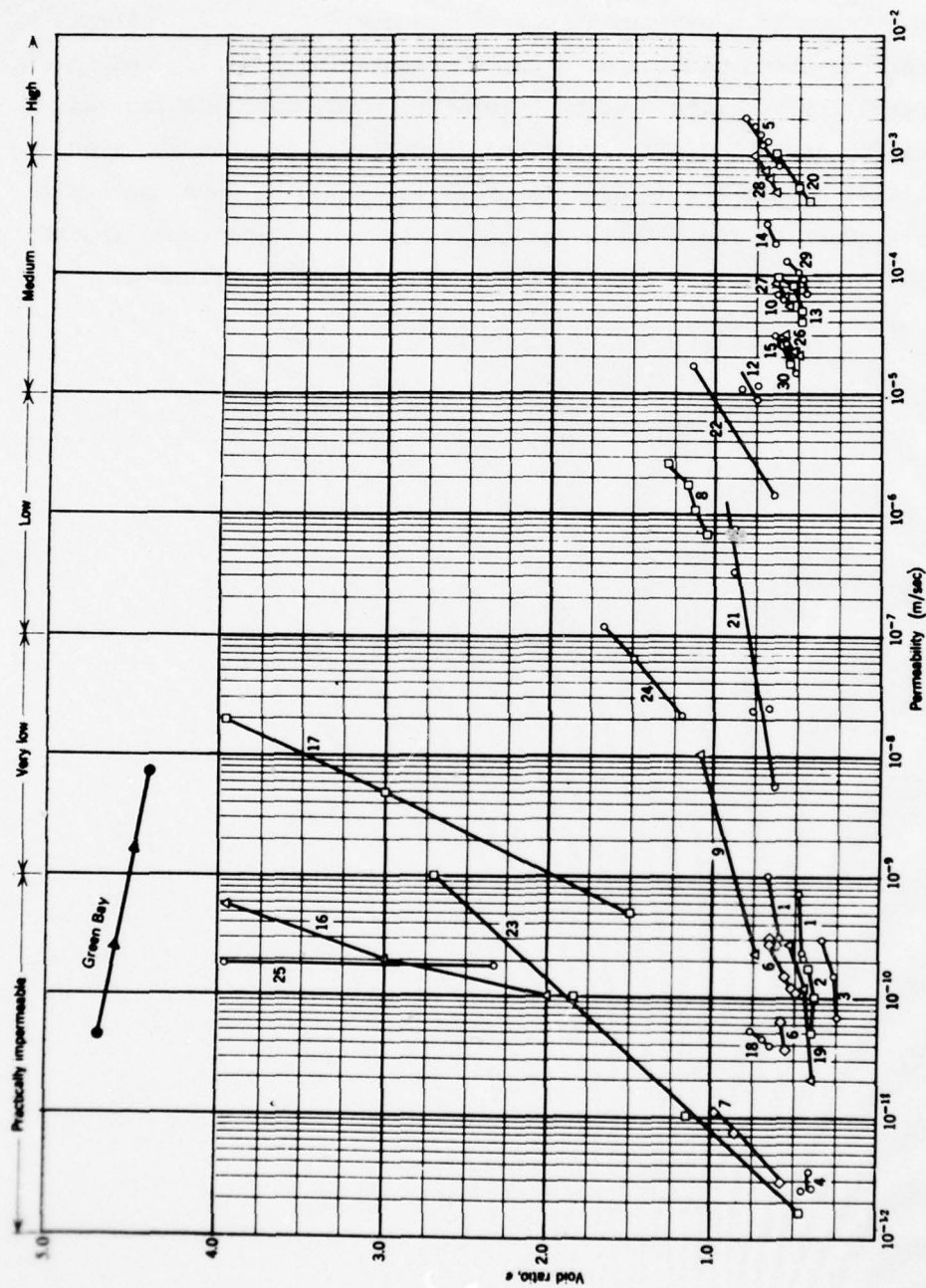Figure 60. Permeability vs void ratio for the O'Brien Lock material

Figure 61. Permeability vs void ratio for the Green Bay material

77

natural desiccation. The time required could be as little as 1 percent of the time required for natural consolidation.

95. There is a certain amount of speculation in this analysis of enhancing the consolidation of dredged material by freezing and thawing. The reliability of extrapolating laboratory thaw consolidation and permeability data to field situations is unproven and the costs and capabilities of pumping dredged material and removing snow uncertain. Only by conducting field tests can these factors be evaluated and the potential of freeze-thaw consolidation enhancement ascertained.

REFERENCES

Bishop, S. L. and Fulton, G. P., "Lagooning and Freezing for Disposal of Water Plant Sludge," Public Works, Vol 99, No. 6, Jun 1968, pp 94-96.

Bruce, A., Clements, G. S., and Stephenson, R. A., "Further Work on the Sludge Freezing Process," The Surveyor, Vol 112, No. 3222, 5 Dec 1953, pp 849-850.

Clements, G. S., Stephenson, R. J., and Regan, C. J., "Sludge Dewatering by Freezing with Added Chemicals," Journal, Institute of Sewage Purification, Part 4, 1950, pp 318-337.

Doe, P. W., Benn, D., and Bays, L. R., "The Disposal of Washwater Sludge by Freezing," Journal, Institution of Water Engineers, Vol 19, No. 4, Jun 1965, pp 251-291.

Farrell, J. B. et al., "Natural Freezing for Dewatering of Aluminum Hydroxide Sludges," Journal, American Waterworks Association, Vol 62, No. 12, Dec 1970, pp 787-791.

Johnson, S. J. et al,., "State-of-the-Art Applicability of Conventional Densification Techniques to Increase Disposal Area Storage Capacity," Technical Report S-77-4, Apr 1977, U. S. Army Engineer Waterways Experiment Station, CE, Vicksburg, Miss.

Katz, W. J. and Mason, D. G., "Freeze Methods Used to Condition Activated Sludge," Water and Sewage Works, Vol 117, No. 4, Apr 1970, pp 110-114.

Kersten, M. S., "Laboratory Research for the Determination of the Thermal Properties of Soil," Final Report, Jun 1949, U. S. Army Engineer District, St. Paul, CE, St. Paul, Minn.

Lambe, T. W. and Whitman, R. V., Soil Mechanics, Wiley, New York, 1969.

Malyshev, M. A., "Deformation of Clays During Freezing and Thawing," Translation 388, 1973, U. S. Army Cold Regions Research and Engineering Laboratory, Hanover, H. H. (Translation of Inzhenerno-Stroitel nyi Institut, S Bornik Nauchnykh Trudov, Vol 14, 1969, pp 58-62.)

Martin, R. T., "Rhythmic Ice Banding in Soil," Bulletin 218, pp 11-23, 1959, National Research Council, Highway Research Board, Washington, D. C.

Morgenstern, N. R. and Smith, L. B., "Thaw-Consolidation Tests on Remoulded Clays," Canadian Geotechnical Journal, Vol 10, No. 1, Feb 1973, pp 25-40.

Nixon, J. F. and Morgenstern, N. R., "The Residual Stress in Thawing Soils," Canadian Geotechnical Journal, Vol 10, 1973, pp 571-580.

Noda, S. et al., "Experimental Studies on Dewatering of Digested Sludge by Freezing, Thawing, and Filtration Method," Journal, Department of Sanitary Engineering, Hokkaido University, No. 9, 1964, pp 41-53.

Office, Chief of Engineers, Department of the Army, "Calculation Methods for Determination of Depths of Freeze and Thaw in Soils," Technical Manual TM 5-852-6, Jan 1966, Washington, D. C.

Ponomarev, V. D., "Experimental Study of the Stress-Strain State of Thawing Bearing Soils," Translation 289, 1971, U. S. Army Cold Regions Research and Engineering Laboratory, Hanover, N. H. (Translated from the Russian, 1966.)

Shusherina, Y. P., "Variation of Physico-Mechanical Properties of Soils Under the Action of Cyclic Freeze-Thaw," Translation 255, 1971, U. S. Army Cold Regions Research and Engineering Laboratory, Hanover, N. H. (Translated from the Russian, 1959.)

Stuart, J. G., "Consolidation Tests on Clay Subjected to Freezing and Thawing," Stockholm, Statens Geotekniska Institut, Saerkryck och Preliminara Rapporter, No. 7, 1964, pp 1-9.

Taylor, D. W., Fundamentals of Soil Mechanics, Wiley, New York, 1948.

Terzaghi, K. and Peck, R., Soil Mechanics in Engineering Practice, 2d ed., Wiley, New York, 1962.

Tice, A. R., Anderson, D. M., and Banin, A., "The Prediction of Unfrozen Water Contents in Frozen Soils from Liquid Limit Determinations," Report 76-8, Apr 1976, U. S. Army Cold Regions Research and Engineering Laboratory, Hanover, N. H.

Tsytovich, N. A., Grigor'eva, V. G., and Zaretskii, J. K., "Study of Consolidation of Thawing Ice-Saturated Grounds," Translation 164, 1970, U. S. Army Cold Regions Research and Engineering Laboratory, Hanover, N. H. (Translated from the Russian, 1966.)

APPENDIX A: COST ANALYSIS

Trenching Costs

1. Assume

   a. Disposal area A_d = 278770 m^2 of width w_d = <u>305 m</u> and length l_d = <u>914 m</u>

   b. Potential volumetric strain ε_v = 17.5 percent

   c. Desirable degree of consolidation U = 90 percent

   d. Maximum trench depth D = <u>1.52 m</u>

   e. Traverse velocity V_t is a function of trench depth as follows:

D, m	V_t, m/hr
0.30	600
0.60	300
0.91	200
1.22	150
1.52	120

   f. Trenches are spaced S at 7.6-m intervals

   g. Trenches run width of site, intercepted by side trenches

   h. Trenching machine costs R_t are $40/hr including rental, operation, and operator costs

   i. Trench depth equals frost depth

2. Length l_t of trench to be cut

$$l_t = A_d/S + w_d + 2\ l_d$$

$$= \underline{278770 \text{ m}^2/7.6 \text{ m} + 305 \text{ m} + 2 \times 914 \text{ m}}$$

$$= \underline{38813 \text{ m}}$$

3. Volume of storage gain attributed to trenching V_{st}

$$V_{st} = A_d \times D \times \varepsilon_v \times 10^{-2} \times U \times 10^{-2}$$

$$= 278770 \text{ m}^2 \times D \times 0.175 \times 0.90$$

$$= 43906 \times D \text{ m}^3$$

4. Cost of trenching per cubic meter of storage volume obtained C_{st}

$$C_{st} = (1_t \times R_t)/(V_t \times V_{st})$$

$$= (38813 \text{ m} \times \$40/\text{hr})/(V_t \times 43906 \times D)$$

$$= 35.230/(V_t \times D)$$

Trench Depth D, m	Traverse Velocity V_t, m/hr	Storage Volume V_{st}, m³	Storage Costs $/m³
0.30	600	13,172	0.20
0.60	300	26,344	0.20
0.91	200	39,954	0.19
0.21	150	53,565	0.19
1.52	120	66,737	0.19

Pumping Costs

5. Assume

a. Disposal area A_d = 278770 m² of width w_d = 305 m and length l_d = 914 m

b. Potential volumetric strain ε_v = 17.5 percent

c. Desirable degree of consolidation U = 90 percent

d. One 75-mm lift T_1 per 40-hr week

A2

$\underline{e}$. Pumping capacity $Q_p = \underline{1.5 \text{ m}^3}/\text{min-pump}$

$\underline{f}$. Cost of 2 laborers or operators $R_l = \$15/\text{hr}$

$\underline{g}$. Cost of pump rental and operation $R_p = \$55/\text{day-pump}$

6. Pump requirements

$\underline{a}$. Volume to be pumped per 75-mm lift V_p

$$V_p - T_l \times A_d = 0.075 \text{ m} \times 278770 \text{ m}^2$$

$$= \underline{20,908 \text{ m}^3}$$

$\underline{b}$. Pumping capacity required Q

$$Q = V_p/1 \text{ week}$$

$$= 20,908 \text{ m}^3/(40 \text{ hr} \times 60 \text{ min/hr})$$

$$= \underline{8.712 \text{ m}^3/\text{min}}$$

$\underline{c}$. Number of pumps required N

$$N = Q/Q_p = (8.712 \text{ m}^3/\text{min})/(1.5 \text{ m}^3/\text{min-pump})$$

$$= 5.81 \text{ pumps}$$

Use $N = \underline{6 \text{ pumps}}$

7. Cost of pump operation per 75-mm lift P_c

$\underline{a}$. Pump rental and operation

6 pumps × 5 days × \$55/day-pump = \$1650

$\underline{b}$. Labor

2 laborers × 40 hr × \$15/hr-laborer = \$1200

$$P_c = \$2850$$

A3

8. Volume of storage gain attributed to pumping V_{sp}

$$V_{sp} = V_p \times \varepsilon_v \times 10^{-2} \times U \times 10^{-2}$$

$$= 20,908 \text{ m}^3 \times 0.175 \times 0.90$$

$$= 3293 \text{ m}^3$$

9. Cost of storage volume gained attributed to pumping C_{sp}

$$C_{sp} = P_c/V_{sp}$$

$$= \$2850/3293 \text{ m}^3$$

$$= \underline{0.87} \ \$/\text{m}^3$$

Snow Removal Costs

10. Assume

    <u>a</u>. Disposal area $A_d = 278770 \text{ m}^2$ of width $w_d = 305$ m and length $l_d = 914$ m

    <u>b</u>. Potential volumetric strain $\varepsilon_v = 17.5$ percent

    <u>c</u>. Desirable degree of consolidation $U = 90$ percent

    <u>d</u>. 9080-kg road grader with 3.7-m-wide blade at a cost $R_g = \$280/\text{day}$

    <u>e</u>. Grader operating velocity $V_g = 3.2$ km/hr

    <u>f</u>. 2.5-m-wide passes w_p

    <u>g</u>. 2 passes per site to remove one 150-mm snowfall

    <u>h</u>. X = depth of freeze, ft

11. Time t_s required to remove one 150-mm snowfall

A4

$$t_s = A_d/(w_p \times 2 \times V_g)$$

$$= 278770 \text{ m}^3/(2.5 \text{ m} \times 2 \times 3.2 \text{ km/hr})$$

$$= \underline{70 \text{ hr/150-mm snowfall}}$$

use $t_s = 80$ hr or 10 8-hr days/150-mm snowfall

12. Cost R_s for removal of one 150-mm snowfall

$$R_s = t_s \times R_g$$

$$= (10 \text{ days/150-mm snowfall}) \times (\$280/\text{day})$$

$$= \underline{\$2800/150\text{-mm snowfall}}$$

13. Volume of storage gain attributed to snow removal V_{ss}

$$V_{ss} = A_d \times X \times \varepsilon_v \times 10^{-2} \times U \times 10^{-2}$$

$$= 278770 \text{ m}^2 \times 0.175 \times 0.90 \times X$$

$$= \underline{43906 \times X}$$

14. Cost of storage gain attributed to snow removal C_{ss}

$$C_{ss} = R_s/V_{ss} = (\$2800/150\text{-mm snowfall})/V_{ss}$$

Freeze Frost Depth X, m	Storage Volume Gain V_{ss}, m^3	Cost C_{ss}, \$/m^3/150-mm Snowfall
0.30	13,172	0.21
0.60	26,344	0.11
0.91	39,954	0.07
1.21	53,126	0.05
1.52	66,737	0.04

A5

APPENDIX B: NOTATION

a area of burette

a_v coefficient of compressibility

A area of test sample

A_d area of disposal site

c_v coefficient of consolidation

C_{sp} cost of storage volume gain attributed to pumping

C_{ss} cost of storage volume gain attributed to snow removal

C_{st} cost of storage volume gain attributed to trenching

D drainage trench depth

e void ratio

F air freezing index

G_s specific gravity of solids

H sample thickness

k permeability

K thermal conductivity of soil

l_d length of disposal area

l_t length of drainage trench to be cut

L volumetric latent heat of fusion

LL liquid limit

MAT mean annual temperature

n conversion factor for air index to surface index

nF surface freezing index

N number of pumps required

p total stress

$\bar{p}, '_o$ effective stress

P_c total pump costs per 75-mm lift

P_f final transducer pressure

P_o initial transducer pressure

PI   plasticity index

PL   plastic limit

Q   total pumping capacity required

Q_p pumping capacity of one pump

R_g costs operating road grader

R_l labor costs

R_p pumping costs

R_s snow removal costs per 150-mm snowfall

R_t trenching machine costs

S   distance between drainage trenches

t   time

t_s time required to remove one 150-mm snowfall

T   mean annual site temperature

T_{avg} average temperature

T_l thickness of disposal lift

T_v time factor related to degree of consolidation

U   degree of consolidation

V   volume of element in percent of total

V_g velocity of road grader

V_t traverse velocity of trenching machine

V_p volume to be pumped

V_{sp} storage volume gain attributed to pumping

V_{ss} storage volume gain attributed to snow removal

V_{st} storage volume gain attributed to trenching

w water content

w_d width of disposal area

w_f frozen water content

w_o organic control

w_p width of road grader passes

X depth of freeze

Z depth of material

γ_b buoyant unit weight of soil

γ_d dry unit weight

γ_{df} final dry density

γ_{di} initial dry density

γ_w unit weight of water

Δt time interval

ε_v volumetric strain

λ coefficient that takes into account mean annual site temperature, surface freezing index, length of freezing season, volumetric latent heat of fusion, and volumetric heat capacity of the soil

σ log total stress

σ'_o residual effective stress

ω_u unfrozen water content